Lebanese American University

The Role of StarD13 in Prostate Cancer Proliferation, Motility, and Invasion

By

Leila Jaafar

A thesis submitted in partial fulfillment of the requirements for the degree of Master of Science in Molecular Biology

School of Arts and Science

May 2020

LAU
الجامعة اللبنانية الأميركية
Lebanese American University

THESIS APPROVAL FORM

Student Name: Leila Jaafar I.D. #: 201706441

Thesis Title: The Role of StarD13 in Prostate Cancer Proliferation, Motility and Invasion

Program: MS in Molecular Biology

Department: Natural Sciences

School: Arts and Sciences

The undersigned certify that they have examined the final electronic copy of this thesis and approved it in Partial Fulfillment of the requirements for the degree of:

Master of Science in the major of Molecular Biology

Thesis Advisor's Name: Mirvat El Sibai

Signature: [redacted] Date: 13 / 05 / 2020
Day Month Year

Committee Member's Name: Roy Khalaf

Signature: [redacted] Date: 13 / 05 / 2020
Day Month Year

Committee Member's Name: Michella Ghassibe-Sabbagh

Signature: [redacted] Date: 13 / 05 / 2020
Day Month Year

LAU
الجامعة اللبنانية الأميركية
Lebanese American University

THESIS COPYRIGHT RELEASE FORM

LEBANESE AMERICAN UNIVERSITY NON-EXCLUSIVE DISTRIBUTION LICENSE

By signing and submitting this license, you (the author(s) or copyright owner) grants the Lebanese American University (LAU) the non-exclusive right to reproduce, translate (as defined below), and/or distribute your submission (including the abstract) worldwide in print and electronic formats and in any medium, including but not limited to audio or video. You agree that LAU may, without changing the content, translate the submission to any medium or format for the purpose of preservation. You also agree that LAU may keep more than one copy of this submission for purposes of security, backup and preservation. You represent that the submission is your original work, and that you have the right to grant the rights contained in this license. You also represent that your submission does not, to the best of your knowledge, infringe upon anyone's copyright. If the submission contains material for which you do not hold copyright, you represent that you have obtained the unrestricted permission of the copyright owner to grant LAU the rights required by this license, and that such third-party owned material is clearly identified and acknowledged within the text or content of the submission. IF THE SUBMISSION IS BASED UPON WORK THAT HAS BEEN SPONSORED OR SUPPORTED BY AN AGENCY OR ORGANIZATION OTHER THAN LAU, YOU REPRESENT THAT YOU HAVE FULFILLED ANY RIGHT OF REVIEW OR OTHER OBLIGATIONS REQUIRED BY SUCH CONTRACT OR AGREEMENT. LAU will clearly identify your name(s) as the author(s) or owner(s) of the submission, and will not make any alteration, other than as allowed by this license, to your submission.

Name: Leila Jaafar

Signature: [redacted] Date: 15 / 05 / 2020
Day Month Year

LAU
الجامعة اللبنانية الأميركية
Lebanese American University

PLAGIARISM POLICY COMPLIANCE STATEMENT

I certify that:

1. I have read and understood LAU's Plagiarism Policy.
2. I understand that failure to comply with this Policy can lead to academic and disciplinary actions against me.
3. This work is substantially my own, and to the extent that any part of this work is not my own I have indicated that by acknowledging its sources.

Name: Leila Jaafar

Signature: [redacted]

Date: 15 / 05 / 2020
Day Month Year

Dedication Page

To the strong and gentle souls that supported my journey,

my loving parents, sisters, and Zeinab.

Acknowledgments

First and above all, I thank God for giving me the strength and determination to finish this journey.

I am grateful for the encouragement of my parents, sisters, grandparents, and friends, especially Zeinab Sweid that supported me tremendously in every step of the way. I would not have done it without their love and prayers.

I would like to thank my mother in science, my mentor, dr. Mirvat El-Sibai that believed in me and pushed me to accomplish this thesis and beyond. I will never forget her support and guidance throughout my three years in graduate school, and I will take it with me wherever I end up in my academic and personal journey.

I would also like to extend my appreciation to the Dean of Arts and Science and all the faculty members especially dr. Michella Ghassibe Sabbagh and dr. Roy Khalaf for their assistance and encouragement as my thesis committee members.

Special appreciation to the members of the EL-Sibai lab that supported me and became my second family throughout my graduate years.

The Role of StarD13 in Prostate Cancer Proliferation, Motility, and Invasion

Leila Jaafar

Abstract

Prostate cancer is one of the most common tumors affecting males. Several risk factors predispose males to develop prostate cancer including age, ethnicity, and dietary habits. Even though it is easy to treat prostate cancer patients in the early stages, the danger of this disease resides in its being metastatic. Metastasis is a defining feature of invasive cancers, a process that includes invading the underlying matrix and migration of cells from the primary tumor to a distant location where they adhere and proliferate to form a new cancerous mass. Metastasis depends on the regulation of actin cytoskeleton dynamics established mainly by the family of Rho GTPases. Rho GTPases alternate between an active GTP-bound and inactive GDP-bound forms, which is accomplished by two classes of regulators, Rho GEFs that activate Rho GTPases by exchanging GDP with a GTP, and Rho GAPs that induce the hydrolysis of GTP into GDP rendering the Rho GTPases inactive. Among the Rho GAPs is StarD13, also called DLC2. In previous studies done at our lab, StarD13 is found to be a tumor suppressor in several tumor types like astrocytoma and breast cancer. In this study, we elaborated on the role of StarD13 in prostate cancer cellular proliferation, adhesion, invasion, and motility. We found that, in prostate cancer, StarD13 is underexpressed and it acts as a suppressor of tumor proliferation, adhesion, and invasion, however, StarD13 is a positive regulator of prostate cancer 2D motility.

Keywords: StarD13, Rho GAP, Rho GTPases, Prostate cancer, Proliferation, Metastasis.

Table of Content

Chapter **Page**

List of Figures ..... **x**

List of Tables ..... **xi**

List of Abbreviations ..... **xii**

Chapter 1 Literature Review **1**

1.1 Cancer **1**

1.1.1 Definition and Classification 1

1.1.2 Initiation and Progression of Cancer 2

1.2 Prostate Cancer **4**

1.2.1 Epidemiology 4

1.2.2 Classification 5

1.3 Cancer Metastasis **7**

1.3.1 Cell Motility 9

1.3.2 Cell Invasion (3D Cell Motility) 10

1.4 Family of Rho GTPases **12**

1.4.1 Definition 12

1.4.2 Rho GTPase Upstream Regulators Include StarD13 12

1.4.3 Rho GTPase Downstream Effector 15

1.5 Aim of this Study **18**

Chapter 2 Materials and Methods **20**

2.1 Functional Comparative Analysis **20**

2.2 Cell Culture **20**

2.3 Antibodies and Reagents **20**

2.4 Immunohistochemistry **21**

2.5 Cell Transfection with siRNA **22**

2.6 Western ImmunoBlotting **22**

2.7 Sphere Formation Assay **23**

2.8 Sphere Immunoblotting **23**

2.9 Proliferation Assay **24**

2.10 Motility Assay (Time-Lapse) **24**

2.11 Wound Healing Assay **25**
2.12 Adhesion Assay **25**
2.13 Immunocytochemistry **26**
2.14 Gelatin Invadopodia Assay **26**
2.15 Quantification of Spheres **26**
2.16 Quantification of Focal Adhesions **27**
2.17 Statistical Analysis **27**
Chapter 3 Results **28**
3.1 StarD13 Regulates Several Proteins and Cellular Processes **28**
3.2 StarD13 is Involved in Many Cellular Pathways **30**
3.3 StarD13 is Under Expressed in Prostate Cancer **31**
3.4 Silencing StarD13 by siRNA **32**
3.4.1 StarD13 Silencing in 2D DU145 Cell Culture 32
3.4.2 StarD13 Silencing in 3D DU145 Cell Culture 33
3.5 StarD13 is a Tumor Suppressor **34**
3.5.1 StarD13 Suppresses Du145 Cell Proliferation 34
3.5.2 StarD13 Reduces Du145 Sphere Formation Rate 35
3.6 StarD13 is Required in Prostate Cancer Motility **36**
3.6.1 Effect of StarD13 on Cell Motility Measured by Time Lapse 36
3.6.2 Effect of StarD13 on Cell Motility Measured by Wound-Healing Assay 37
3.7 StarD13 is a Negative Regulator of Prostate Cancer Adhesion **38**
3.7.1 StarD13 Reduces Overall Adhesion of DU145 Cells 38
3.7.2 StarD13 Reduces Focal Adhesions Count and Area 39
3.8 StarD13 is a Negative Regulator of Prostate Cancer Invasion **40**
Chapter 4 Discussion **42**
Chapter 5 Conclusion **46**
References **47**

List of Figures

Figure **Page**

Figure 1. Mutator Phenotype Hypothesis.....2
Figure 2. Cancer Stem Cell Hypothesis.....3
Figure 3. The Hallmarks of Cancer.....4
Figure 4. Gleason Score for Prostate Cancer Grading.....6
Figure 5. Steps of Cancer Metastasis.....8
Figure 6. Cell Motility Cycle.....10
Figure 7. Lamellipodia, filopodia, and Invadopodia.....11
Figure 8. Rho GTPase Activity Regulation.....13
Figure 9. StarD13 Amino Acid Domains.....14
Figure 10. Pathways Modulated by StarD13 Through Rho GTPases.....18
Figure 11. Biological Functions of StarD13 Targets.....29
Figure 12. Biological Processes Performed by StarD13 Targets.....29
Figure 13. StarD13 Targets are Involved in Various Biological Pathways.....30
Figure 14. Networks Involving StarD13 and its Targets.....31
Figure 15. StarD13 is Under Expressed in Prostate Cancer.....32
Figure 16. Efficient Depletion of StarD13 by si-RNA.....33
Figure 17. StarD13 is Silenced in DU145 Spheres by si-RNA.....34
Figure 18.StarD13 Reduces Du145 Cell Proliferation in 2D Culture.....35
Figure 19. StarD13 Reduces DU145 Sphere Area.....37
Figure 21. StarD13 Depletion Induces Wound Closure.....38
Figure 22. StarD13 is a Negative Regulator or DU145 Cell Adhesion to Collagen.....39
Figure 23. StarD13 Negatively Regulates Paxillin in Du145 Cells.....40
Figure 24 StarD13 Silencing Enhances DU145 Cell Invasion.....41

List of Tables

Table **Page**

Table 1.StarD13 Targets Proteins in Several Tumor Types. 28

List of Abbreviations

AJCC: American Joint Committee on Cancer

UICC: Union of International Cancer Control

PSA: Prostate-Specific Antigen

TNM: Tumor, Node, Metastasis

EMT: Epithelial-to-Mesenchymal Transition

Rho: Ras homologous

GTPase: Guanosine triphosphatase

ECM: Extracellular matrix

MMP: Matrix metalloproteinase

Cdc42: Cell division cycle 42

Arp2/3: Actin-related protein 2/3

Rac1: Ras-related C3 botulinum toxin substrate 1

GTP: Guanosine triphosphate

GDP: Guanosine diphosphate

GEF: Guanine Nucleotide Exchange Factor

GAP: GTPase Activating Protein

GDI: Guanine Nucleotide Dissociation Inhibitor

DLC: Deleted in Liver Cancer

StarD13: Steroidogenic Acute Regulatory Protein-Related Lipid Transfer Domain Containing Protein 13

SAM: Sterile Alpha Motif

FAT: Focal Adhesion Targeting

Bax: BCL2-Associated X Protein

BMF: Bcl-2 Modifying Factor

ROCK: Rho Kinase

WASP: Wiskott-Aldrich Syndrome Protein

MAPK: Mitogen-Activating Protein Kinase

mDia: Mammalian Homolog of Diaphanous

FMNL: Formin Like Protein

LIMK: LIM Kinase

WAVE: WASP-Family Verprolin-Homologous

Rho A: Ras homologous member A

Rho C: Ras homologous member C

Rho G: Ras homologous member G

VEGF: Vascular Endothelial Growth Factor

ERK: Extracellular Signal-regulated Kinase

PANTHER: Protein Analysis Through Evolutionary Relationship

STRING: Search Tool for the Retrieval of Interacting Genes/Proteins

ATCC: American Type Culture Collection

RPMI: Roswell Park Memorial Institute

FBS: Fetal Bovine Serum

Tks-4: Tyrosine Kinase Substrate 4

siRNA: Small interfering Ribonucleic Acid

SDS-PAGE: Sodium Dodecyl Sulfate Polyacrylamide Gel Electrophoresis

PVDF: Polyvinylidene fluoride

PBS: Phosphate Buffered Saline

ECL: Enhanced Chemiluminescence

BSA: Bovine Serum Albumin

PFA: Paraformaldehyde

WST-1: Water Soluble Tetrazolium Salts

HEPES: 4-(2-hydroxyethyl)-1-piperazineethanesulfonic acid

HRP: Horse Radish Peroxidase

DAPI: 4′,6-diamidino-2-phenylindole

ROI: Region of Interest

ELISA: Enzyme-Linked Immunosorbent Assay

Chapter 1

Literature Review

1.1 Cancer

1.1.1 Definition and Classification

According to the National Cancer Institute, cancer is defined as the disease caused by uncontrolled cell proliferation and skipping programmed cell death due to cell cycle dysregulation. This phenomenon, according to the American Cancer Society, leads to the formation of masses of abnormal cells among normal ones which alters a normal body function.

In 2020, it is estimated that, in the United States, there will be 1.8 million newly diagnosed cancer cases and 606,520 deaths (Cancer facts & figures 2020 | american cancer society.). This disease affects all ages from infants to older patients, and its causes, although not fully identified yet, vary from genetic, health-related like obesity or lifestyle, to external environmental factors.

Cancer tumors are classified into two groups, benign (non-malignant) and malignant tumors. While a cancerous mass may be an overlap of both tumor groups in some cases (Cerroni et al., 2010), malignant tumors tend to be invasive to surrounding tissue, and lymphatic and blood vessels which permit their metastatic ability (Idikio, 2011).

1.1.2 Initiation and Progression of Cancer

Genetic mutations are, in most cases, at the base of tumor formation. These primary mutations are spread all over the genome and they usually occur in genes that are responsible for DNA stability (Loeb, Lawrence A., Loeb, & Anderson, 2003). Altering the genetic stability leads to the generation of new mutation all over the genome including mutations that activate oncogenes and inactivate tumor suppressor genes. These mutations give the cell growth advantage over the surrounding normal cells. This is the "Mutator Phenotype Hypothesis" postulated by Loeb and his colleagues in 1974 to explain tumor initiation and heterogeneity and its effect on cancer treatment (Loeb, L. A., Springgate, & Battula, 1974).

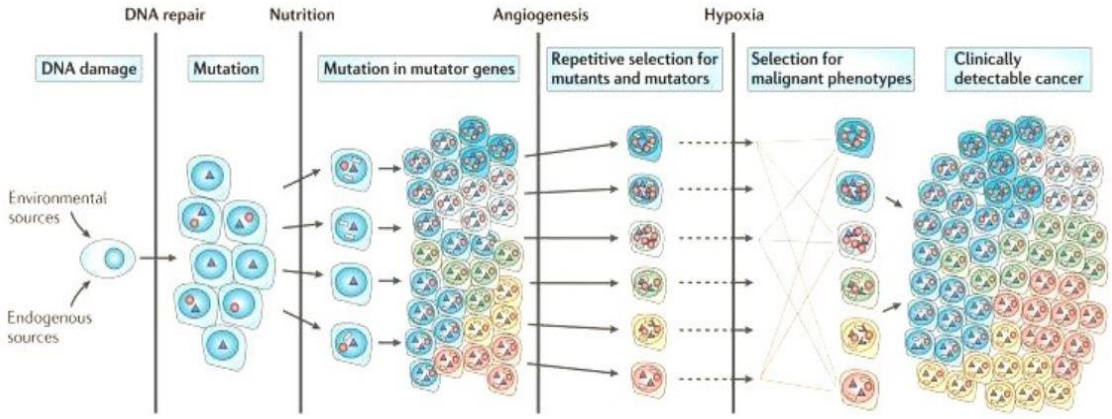

Figure 1. Mutator Phenotype Hypothesis. A primary mutation in response to environmental factors or endogenous alterations may destabilize the genome and lead to the accumulation of mutations leading to the formation of tumors. Image is adopted and modified from (Loeb, Lawrence A., 2011)

However, this model requires long-lived cells that encompass all the mutations and at the same time give rise to differentiated cancer cells forming the tumor, which is the self-renewal property present at the core of cancer development. This concept of "Cancer Stem Cell" is one of the

first posits that elaborated on the origin of cancer (Tan, Park, Ailles, & Weissman, 2006)

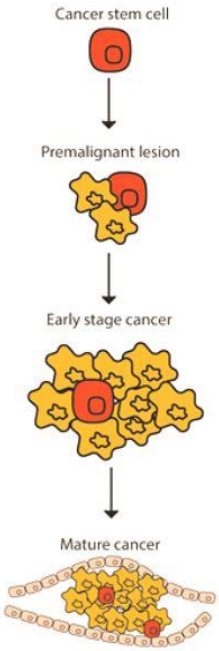

Figure 2. Cancer Stem Cell Hypothesis. Cancer stem cell originate cancer cells which leads to the formation of a mature tumor. This figure is adopted and modified from (Bajaj, Diaz, & Reya, 2020).

Regardless of the origin of cancer, the development of malignant properties of a tumor also called tumorigenesis, is the notion that most scientists agree on. Tumorigenesis includes cellular dedifferentiation, rapid proliferation, apoptosis evasion, metastasis, immune system manipulation, angiogenesis, and metabolic and epigenetic alteration. All of these, present the hallmarks of cancer (Hanahan & Weinberg, 2000; Hanahan & Weinberg, 2011).

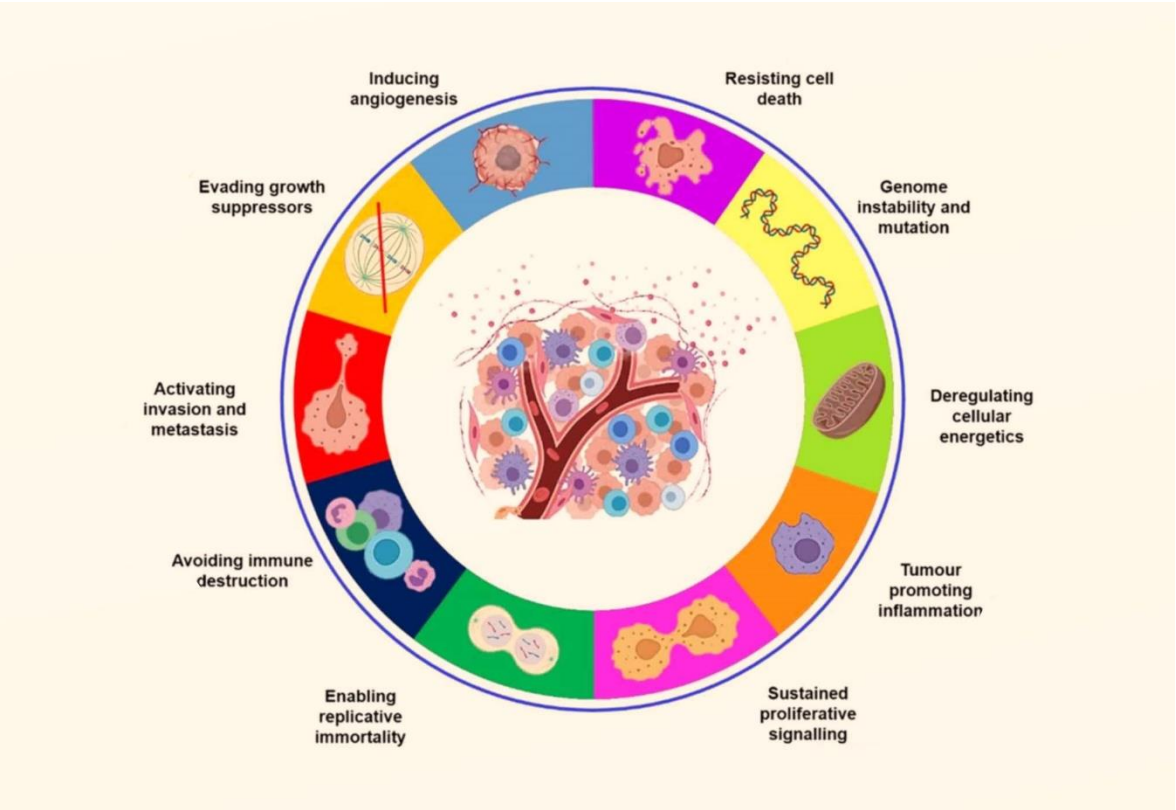

Figure 3. The Hallmarks of Cancer. Cancer malignancy is identified by several hallmarks set by Hanahan and Weinberg. They include, rapid proliferation, escaping apoptosis, induction of angiogenesis and invasion, and metastasis. This figure is adopted and modified from (Garnham, Scott, Livermore, & Munkley, 2019).

1.2 Prostate Cancer

1.2.1 Epidemiology

Prostate cancers, in most of the cases, are adenocarcinomas that occur in the prostate gland present exclusively in males. In rare cases, Sarcomas, small cell carcinomas, and transitional cell carcinomas may also start in the prostate (Cancer facts & figures 2020 | american cancer society.).

Prostate cancer, second to skin cancer, is the most common type of cancer that affects men in the US. In 2020, it is estimated by the American Cancer Society that there will be 191,930 new cases and 33,330 deaths among men from prostate cancer (Key statistics for prostate cancer | prostate cancer facts.).

Prostate cancer risk factors include age where the majority of cases are diagnosed at the age of 66 (Key statistics for prostate cancer | prostate cancer facts.), ethnicity where African American men have a higher probability to develop prostate cancer when compared to Caucasians, surrounding environment, and life habits like high vitamin E diet (Information, National Center for Biotechnology, Pike, U. S. National Library of Medicine 8600 Rockville, MD, & Usa, 2020).

Symptoms of prostate cancer usually occur at advanced stages, and they include blood in semen or urine, elevated urge to urinate, or slow flow of urine which are also symptoms of prostate hypertrophy (Information, National Center for Biotechnology et al., 2020). Prostate cancer is among the tumors with high recovery rates due to its slow growth rate. However, prostate cancer tends to spread to other body parts through the blood or lymph which manifests as other symptoms especially bone pain because the axial skeleton is the major target of this metastatic disease (Rawla, 2019).

1.2.2 Classification

Clinical and pathological staging systems are adopted by the American Joint Committee on Cancer (AJCC) and the International Union Against Cancer (UICC) to identify the grade of prostate cancer. Clinical staging includes, among others, testing for prostate-specific antigen (PSA), and the Gleason score which represents the preferred system for grading prostate cancer. The Gleason score depends on tissue histology and arrangement and the degree of similarity between the tumor biopsy and normal tissue. The scores range from 6 to 10, 6 being the

lowest score corresponding to low-grade tumors, and 10 correspondings to the most aggressive prostate cancer forms (Chen, N. & Zhou, 2016; Cheng, Montironi, Bostwick, Lopez-Beltran, & Berney, 2012).

The TNM system is another important staging system that determines the size and location of the primary tumor, if it has spread to lymph nodes, and whether the tumor has metastasized to other locations. In the TNM system, stages start from stage 0 being an abnormal growth called carcinoma in situ, then stage I indicating a localized tumor, followed by stages II and III being larger masses that has invaded adjacent tissue and lymph nodes, and finally stage IV suggesting a metastatic prostate tumor found in other body locations (Cheng et al., 2012; Ohori, Wheeler, & Scardino, 1994).

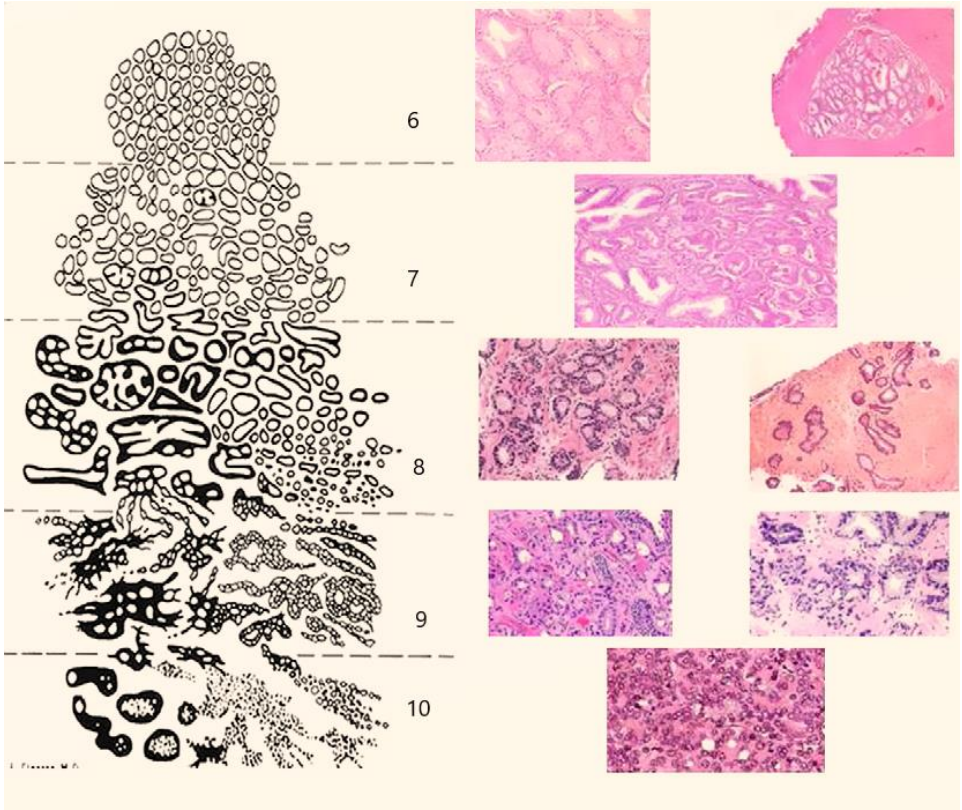

Figure 4. Gleason Score for Prostate Cancer Grading. Gleason score depends on the differences in histological patterns among prostate cancer tissue to determine the tumor grade. The figure is adopted and modified from (Nguyen, Sabata, & Jain, 2012).

1.3 Cancer Metastasis

Cancer tumors are extremely heterogeneous whereby cells of the same tumor show variation in genetic and epigenetic regulations. Added to that, the complexity and heterogeneity of the tumor microenvironment that contains non-cancer cells, nutrients, signaling factors, and the stromal make-up (McGranahan & Swanton, 2017; Yuan, 2016). These facts add to the tumor complexity and lead to variations in the clinical treatment results among patients of the same type of tumor (Dagogo-Jack & Shaw, 2018; Kwak et al., 2015). Among the heterogeneous aspects of tumors that led to the high morbidity rate of this disease, is cancer metastasis (Christofori, 2006; Gupta & Massagué, 2006).

Cancer metastasis is the migration of cancer cells from the primary tumor site to a distant location in the body. This process starts with tumor cells downregulating adhesion proteins and detaching from the primary tumor. This is followed by invading the underlying extracellular matrix reaching blood or a lymphatic vessel. Then these migrating tumor cells interact with the endothelial cells of the vasculature and intravasate into the blood (or lymph) stream that takes it away from the original tumor site. Later on, the metastasizing cells interact again with the endothelial cells of the vessel and extravasate into a different organ where they disseminate and colonize to form a secondary tumor (Zeeshan & Mutahir, 2017). This description also applies to epithelial-to-mesenchymal transition (EMT) performed by normal cells during embryogenesis and wound healing, and that's why it is believed that EMT is a pro-migratory

state that primary cancer cells must acquire to initiate cancer metastasis (Pastushenko & Blanpain, 2019).

Throughout the whole process of metastasis, migrating tumor cells must adapt to changes in the surrounding environment and overcome the immune system to accomplish their mission (Deng et al., 2014; Pantel & Speicher, 2016). Also, the metastasizing cancer cells must regulate their actin cytoskeleton dynamics to enable them to adhere, invade, or migrate when needed. Each of these processes requires different actin-rich structures that are formed as a result of intracellular signaling pathways conducted mainly by the family of Rho GTPases in response to specific (internal and external) signals (Ma et al., 2019; Sousa-Squiavinato, Rocha, Barcellos-de-Souza, de Souza, & Morgado-Diaz, 2019).

Cancer cells perform two main activities to establish metastasis, cell migration, and cell invasion.

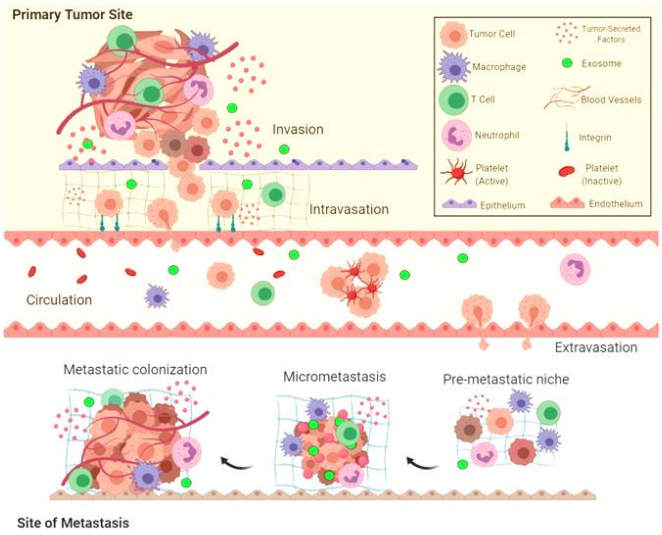

Figure 5. Steps of Cancer Metastasis. Cancer metastasis starts by invasion, intravasation, migration in the circulation, extravasation, and colonization in the new metastatic site. This figure is adopted and modified from (Fares, Fares, Khachfe, Salhab, & Fares, 2020).

1.3.1 Cell Motility

Cell motility is a key process that is performed during cancer metastasis. Initially, it is utilized by many eukaryotic cells for survival, as in the case of single-cell eukaryotes, or to accomplish a variety of important processes such as organogenesis or wound healing in a multicellular organism. Cell motility may be done in two manners, swimming or crawling (Fritz-Laylin, Lord, & Mullins, 2017; Pollard & Borisy, 2003). While swimming is achieved by flagella, crawling movement involves several actin-rich structures that assemble and disassemble rapidly throughout the cell migration course (Carvalho-Santos, Azimzadeh, Pereira-Leal, & Bettencourt-Dias, 2011; Lämmermann & Sixt, 2009).

In mammals, cells move in response to a signal, such as inflammatory response factors for macrophages (Shi et al., 2018). The movement of the cell is a multistep cycle that starts with the detection of the signal by cell membrane receptors which transmit it to the cell interior where the direction of motion is decided. The signal is transduced in a series of pathways that lead to the actin cytoskeleton remodeling at the leading edge of the cell and the formation of cytoplasmic protrusions called lamellipodia and filopodia (Alblazi & Siar, 2015). Then the actin polymers are stabilized by adhering to the substrate through the focal adhesions at the front end of the cell, while the rear end is retracting by detaching the focal adhesions from the extracellular matrix (ECM) (Bailly & Condeelis, 2002; Lauffenburger & Horwitz, 1996; Michaelis, 2014).

Cell motility is a process recycled by cancer cells as a response to pro-metastatic signals such as hypoxia (Hiraga, 2018), and as a mean to resist cancer-targeting treatments (Wu et al., 2013).

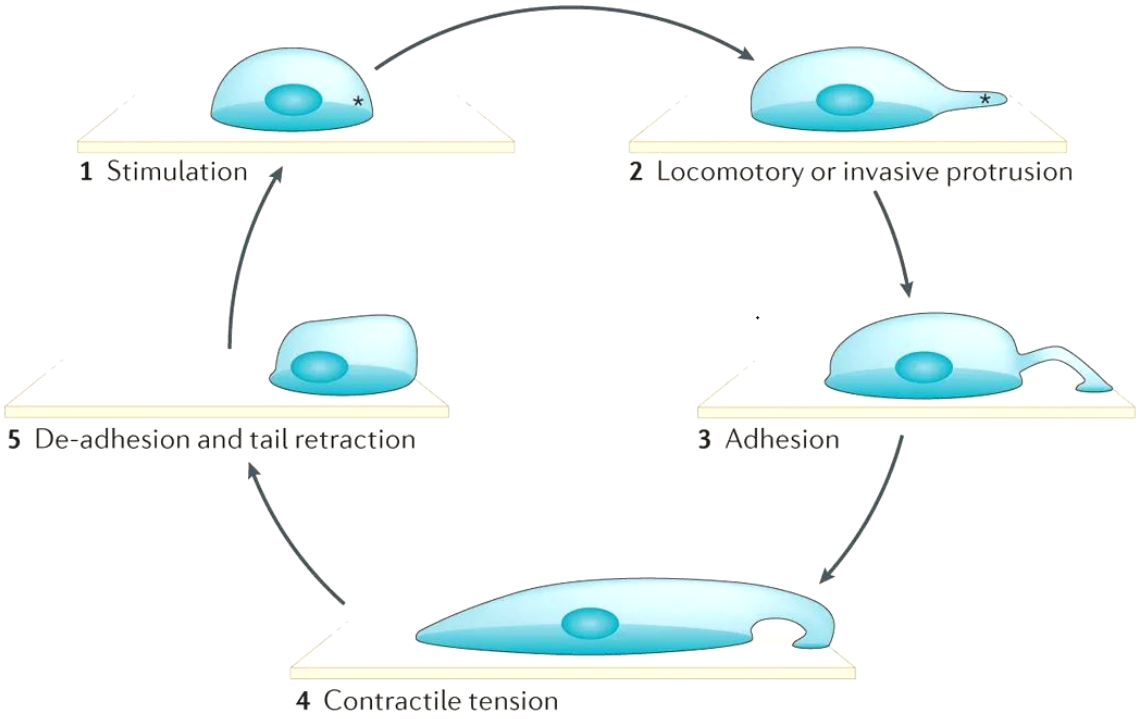

Figure 6. Cell Motility Cycle. Upon the stimulation of cellular migration, the cell extends cytoplasmic protrusion in the direction of the signal then adheres to the substrate to create a contractile tension that leads to the detachment of the adhesive structure in the tail end and the retraction of the cell. The figure is adopted and modified from (Figure 1: Steps of the cell motility cycle. | nature reviews molecular cell biology.)

1.3.2 Cell Invasion (3D Cell Motility)

The second step of cancer metastasis after EMT is invading the underlying extracellular matrix to reach the blood vessel. This process is done by a class of actin-rich cytoplasmic structures called invadopodia (Alblazi & Siar, 2015). Condeelis and his colleagues considered invadopodium to be another hallmark of cancer because it is the main conductor of tumor metastasis (Eddy, Weidmann, Sharma, & Condeelis, 2017).

The invasion process starts by degrading the ECM of the underlying epithelium by the proteolytic activity of invadopodia established by membrane-bound or soluble matrix metalloproteases (MMP) (Kumar, Das, Barai, & Sen, 2018). Then the cell migrates on the ECM of the vascular endothelium before degrading it to intravasate into the lymph or bloodstream (Génot & Gligorijevic, 2014; Murphy & Courtneidge, 2011).

The invadopodium is an actin cytoskeletal structure, and so the Rho GTPase family of proteins has a role in its formation and regulation. Mainly, Cdc42 that maintains an active Arp2/3 complex at the invadopodia core (Beaty & Condeelis, 2014; Bravo-Cordero, Magalhaes, Eddy, Hodgson, & Condeelis, 2013; Sharma et al., 2013). Also, Rho A and Cdc42 positively regulate local ECM degradation through the modulation of MMPs (Jacob & Prekeris, 2015). While Rho A, Rho C, and Cdc42 upregulate invadopodia formation and function, Rac1 encourages invadopodia disassembly (Moshfegh, Bravo-Cordero, Miskolci, Condeelis, & Hodgson, 2015).

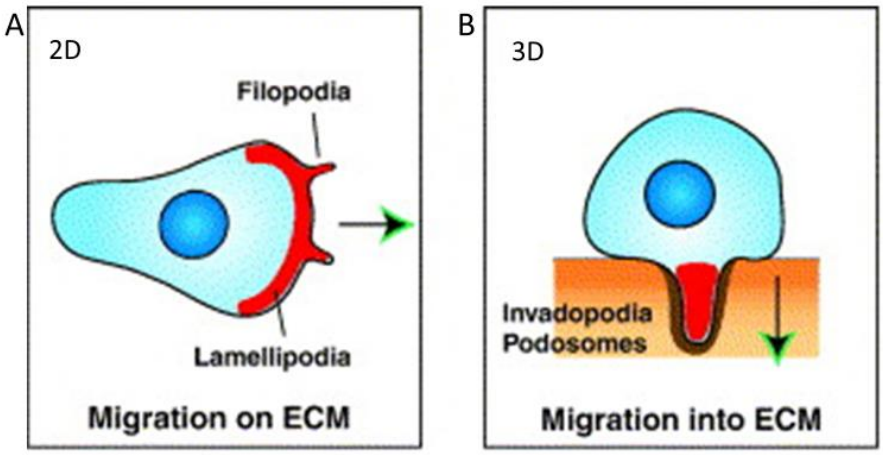

Figure 7. Lamellipodia, filopodia, and Invadopodia. (A) Lamellipodia forms the main cellular protrusion in the direction of 2D motility and from it extend smaller filopodia. (B) Invadopodia degrades the underlying matrix and aids the cell in 3D migration. Image is adopted and modified from (Yamaguchi & Condeelis, 2007).

1.4 Family of Rho GTPases

1.4.1 Definition

The family of Rho GTPases is a part of the Ras superfamily, and it consists of over 20 genes in humans (Vega & Ridley, 2008).

Rho GTPases are admitted to be the main regulators of actin cytoskeleton dynamics and various cellular processes that include cell cycle progression, vesicular trafficking, cell polarity, and cell motility (Heasman & Ridley, 2008). Since this family of proteins is incorporated in such vital aspects of a cell, their dysregulation leads to major consequences including cancer transformation.

1.4.2 Rho GTPase Upstream Regulators Include StarD13

Rho GTPases alternate between an active GTP-bound form and an inactive GDP-bound form. This cycle is achieved by a group of upstream regulators, Rho GEFs, Rho GAPs, and GDIs. While the guanine nucleotide exchange factors (GEFs) catalyze the exchange of GDP with a GTP rendering the Rho GTPase active, GTPase-activating proteins (GAPs) enhances the intrinsic GTPase activity of Rho GTPases which leads to the hydrolysis of the GTP, therefore, inactivating it. Finally, guanine nucleotide dissociation inhibitors (GDIs) binds to the inactive GDP-bound form of Rho GTPases inhibiting them from being activated by Rho GEFs (Ridley, 2011; Rossman, Der, & Sondek, 2005).

Several proteins of the Rho GTPase family are considered as atypical proteins because they are not regulated by the canonical cycling of nucleotide. Rather, these atypical Rho GTPases may have a greater GTP hydrolyzing

capability or minimal cycling of GTP/GDP which renders them constitutively active or inactive, respectively. Atypical Rho GTPases are instead regulated by epigenetic or post-expression modulation by degradation (Dickover et al., 2014; Haga & Ridley, 2016).

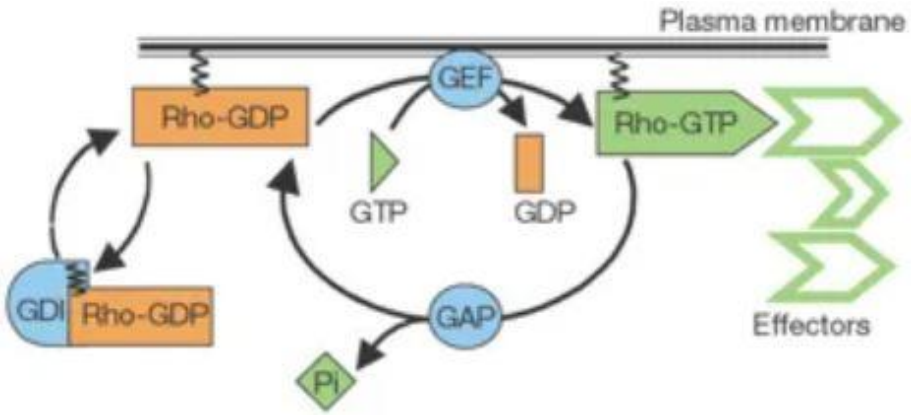

Figure 8. Rho GTPase Activity Regulation. Rho GTPases are activated by GEFs and inactivated by GAPs that enhance their intrinsic GTPase activity. GDIs sequester inactive Rho GTPases and inhibit their interaction with GEFs. The figure is adopted and modified from (Etienne-Manneville & Hall, 2002).

1.4.2.1 StarD13 is a Rho GAP

- *StarD13 Domains:*

StarD13 also called DLC2, is a Rho GAP encoded by the DLC2 gene that is located on chromosome 13 of the human genome. StarD13 protein comprises four amino acid domains each involved in a specific function (Ching et al., 2003).

At the C-terminus, there is the Star-related lipid transfer domain responsible for the transfer of lipid droplets involved in maintaining cellular membranes (Satheesh et al., 2016; Sun, Sun, & Song, 2019).

A second domain is the GAP domain of StarD13 (Ching et al., 2003). This domain, in addition to a small ATP/GTP binding motif (Ching et al., 2003),

allows this protein to negatively regulate several members of the Rho GTPase family that are involved in the modulation of actin cytoskeleton dynamics and cell cycle (El-Sitt & El-Sibai, 2013; Hanna & El-Sibai, 2013).

Another DLC2 domain is the SAM (Sterile Alpha Motif) domain (Sun et al., 2019). This domain functions as a protein and lipid-binding domain which allows StarD13 to bind to several ligands and localizes it to the cytoplasmic membrane (El-Sitt & El-Sibai, 2013; Kwan & Donaldson, 2007).

The fourth domain of StarD13 is the focal adhesion targeting (FAT) domain. FAT binds to Tensin2 which is a key factor of focal adhesions that allow the cell to attach to the underlying substrate. So, it could be said that StarD13 also localizes to focal adhesions due to the presence of the FAT domain (Kawai et al., 2009).

All these domains give StarD13 a wide range of cellular functions rendering this protein crucial for cell proliferation, migration, and cell cycle control. All of these cellular processes are at the core of tumorigenesis (Khalil et al., 2014; Ullmannova & Popescu, 2006).

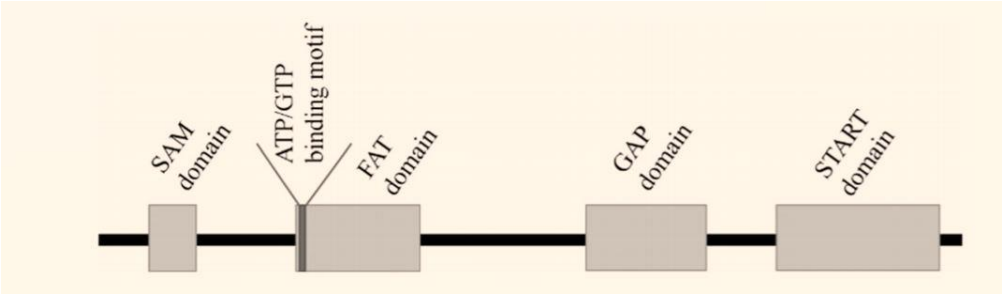

Figure 9. StarD13 Amino Acid Domains. The figure is adopted and modified from (Jaafar, Chamseddine, & El-Sibai, 2020)

- *StarD13 in Cancer:*

StarD13 gene is often underexpressed in many cancer types (El-Sitt et al., 2012; Hanna et al., 2014; Sun et al., 2019; Yang, Z. et al., 2019), this may be due to the deletion of DLC2, epigenetic regulation, or loss of copy number of DLC2 gene encoding StarD13 (Hankins et al., 2008; Tayrac et al., 2009; Wang, Qian, Rajaram, Durkin, & Lowy, 2016).

StarD13 positively regulates pro-apoptotic factors such as caspase-3, Bax, and BMF. When StarD13's activity is lost in tumors, these pro-apoptotic factors are inactivated, and thus cell escapes programmed cell death. This phenomenon is at the core of cancer malignancy (Guo et al., 2018).

Normally, StarD13 inactivates Rho GTPase by its GAP domain, mainly RhoA and Cdc42 (Ching et al., 2003; El-Sitt & El-Sibai, 2013; Kwan & Donaldson, 2007). However, StarD13 is downregulated in tumors which results in increased Rho GTPase activity.

1.4.3 Rho GTPase Downstream Effector

Rho GTPases are incorporated in a huge variety of cellular processes. This involvement is demonstrated by their ability to regulate a wide range of factors downstream from them.

Rho A and Cdc42 are involved in cell migration and invasion, and the dysregulation of Rho GTPase regulators, such as StarD13, in tumors enhances their activity. This results in the activation of the ROCK pathway downstream Rho A that is involved in cell adhesion, actin nucleation, and migration (Basak et al., 2018; Worthylake, Lemoine, Watson, & Burridge, 2001).

Moreover, WAVE is a scaffold protein that, when active, leads to actin nucleation and the formation of lamellipodia through the Arp2/3 complex. WAVE is present downstream Rac1 which is a member of the Rho GTPase family (Ridley, 2011). Also, Cdc42 is a positive regulator of the N-WASP-Arp2/3 axis. This pathway is involved in invadopodia assembly and invasion of the underlying extracellular matrix (Stengel & Zheng, 2011). The degradation of the ECM is catalyzed by metalloproteases MMP2/9 that are also positively regulated by Cdc42 (Yamaguchi, Pixley, & Condeelis, 2006).

Other effectors downstream Rho A and Cdc42 control proliferation and cell cycle progression. One of which is the MAPK pathway that is modulated by Rho A and is responsible for enhancing cell cycle progression (Li, W., Chong, & Guan, 2001).

Added to that, Rho GTPases are present upstream several proteins of the formin family that is associated with the nucleation and elongation of growing actin filaments (Kühn & Geyer, 2014). Active Rho GTPases leads to the activation of formins. The activation of mDia, a formin downstream effector of Rho and Cdc42 (Watanabe et al., 1997; Watanabe, Kato, Fujita, Ishizaki, & Narumiya, 1999), promotes its binding to the actin barbed end and the formation of actin stress fibers and filopodia (Beli, Mascheroni, Xu, & Innocenti, 2008; Higashida et al., 2004). MDia is further involved in spindle positioning and mitotic division which is related to the progression of the cell cycle (Braun & Olayioye, 2015; Vitiello, Ferreira, Maiato, Balda, & Matter, 2014). Also, the activation of FMNL, another formin protein downstream Rho

GTPases (Seth, Otomo, & Rosen, 2006), results in actin severing and bundling and the elongation of lamellipodia and filopodia (Harris, Li, & Higgs, 2004; Yayoshi-Yamamoto, Taniuchi, & Watanabe, 2000).

LIMK is a downstream effector from Rho, Cdc42, and Rac1. LIMK is incorporated in the mitotic spindle and actin dynamics through the inactivation of the family of cofilin by phosphorylation. Cofilin binds to the filaments of actin leading to their disassembly (Bamburg, 1999; Galkin et al., 2011; Gorovoy et al., 2005).

On another note, Rho GTPases play an important role in the production and transmission of angiogenic signals from vascular endothelial growth factors (VEGFs) into the interior of an endothelial cell leading to angiogenesis. Angiogenesis is the process of the formation of new blood vessels and tumors often expedite this process to escape nutrient deficiency and hypoxia (Folkman, 1995; Nicolas, Abdellatef, Haddad, Fakhoury, & El-Sibai, 2019). Several Rho GTPase proteins positively regulate angiogenesis in various ways through the regulation of multiple downstream effectors. Whereby, Rho A activates ROCK that, in addition to its role mentioned above, stimulates angiogenesis, and Rho G that, through the Cdc42-Rac1 axis, leads to the activation of ERK which also results in endothelial angiogenesis (El Atat, Fakih, & El-Sibai, 2019; Zhao et al., 2006).

Rho GTPases are a family of multitasking proteins that are incorporated in various cellular processes; therefore, their tight regulation is a key to ensure the proper running of vital cellular operations.

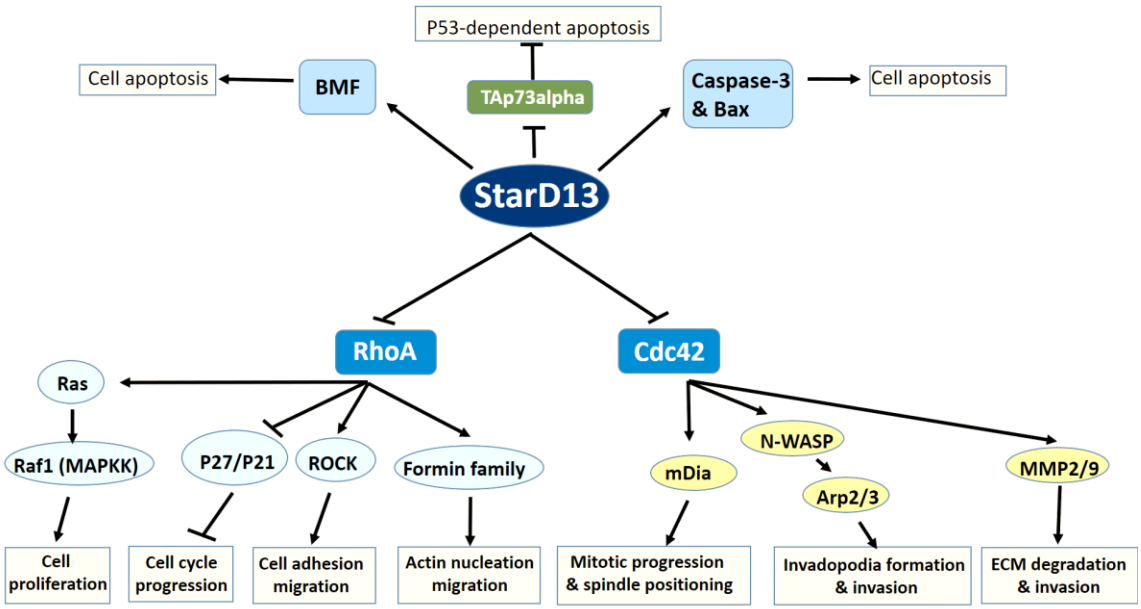

Figure 10. Pathways Modulated by StarD13 Through Rho GTPases. Downstream effectors of StarD13 are involved in cell cycle progression, migration, invasion, and apoptosis. The figure is adopted and modified form (Jaafar et al., 2020).

1.5 Aim of this Study

StarD13 dysregulation is at the core of cancer malignancy, and prostate cancer is one of the top tumors affecting males worldwide, so knowing the role of StarD13 in prostate cancer could be a step towards personalized targeted therapy of this type of tumors.

In this study, we want to assess the overall expression of StarD13 in normal and prostate cancer tissue, and determine the role of StarD13, on prostate cancer proliferation, 2D migration comprising cellular adhesion and motility, 3D motility represented by cell invasion through invadopodia.

On the other hand, since 2D cell culture is not a realistic representation of tumor behavior, we wanted to know the role of StarD13 in prostate cancer spheroids that present 3D culture.

Chapter 2

Materials and Methods

2.1 Functional Comparative Analysis

Functional comparative analysis of protein function and interactions were done by the PANTHER-Gene List Analysis database. The pathways were determined by the STRING database. The minimum required interaction score was set to high confidence (0.7) and the active interaction sources were limited to information fished from textmining, experimentally determined interactions, and curated databases.

2.2 Cell Culture

Human prostate cancer cell line DU145 obtained from ATCC (American Type Culture Collection), was cultured in RPMI-1640 AQ media supplemented with 10% fetal bovine serum (FBS), 1% non-essential amino acids, and 100U penicillin/streptomycin in a humidified chamber at 37°C and 5% CO_2.

2.3 Antibodies and Reagents

The following antibodies were used in this study: Rabbit polyclonal anti-StarD13 antibody, mouse monoclonal anti-actin antibody, and rabbit polyclonal anti-Tks4 antibody were obtained from Abcam. Mouse monoclonal anti-StarD13 antibody and rabbit monoclonal anti-paxillin antibody was purchased from Santa Cruz Biotechnology. Anti-rabbit and anti-mouse HRP-conjugated secondary antibodies were obtained from Promega Co., Wisconsin. Fluorescent secondary anti-rabbit and anti-mouse antibodies (Alexa Fluor 488-green) were obtained from Invitrogen. To

visualize the F-actin cytoskeleton, cells were stained with Rhodamine phalloidin (Red) obtained from Invitrogen. And to visualize the nucleus, DAPI stain (Blue) was purchased from Roche.

2.4 Immunohistochemistry

Paraffin-embedded tissue slides of normal and adenosis of prostate tissues were purchased from Origene. Deparaffinization by xylol was done followed by hydration of the sample by ethanol. The slides were then rinsed under the slow tap to remove all paraffin. Then the slides were hydrated again by placing it in PBS for 20 min at room temperature. Meanwhile, 200-300ml of antigen retrieval buffer (1mM EDTA pH=8) was heated in a 700W microwave for 5 min. The hot retrieval buffer was added to the slides that were heated twice for 5 min in the microwave with a 1 min break and addition of relatively cool retrieval buffer in between. After surrounding the tissues with a water repellent material (clear nail polish), the tissues were blocked by a 4% Blocking solution (PBS+4% BSA+0.1% Triton-X 100) at room temperature. Then the tissue was incubated with mouse monoclonal anti-StarD13 antibody (Santa Cruz; 1:300) for 2 hours. After that, the slides were washed with ice-cold PBS. Secondary anti-mouse antibody coupled to Alexa fluor-488 fluorophore from Invitrogen was added to the slides for 30 min at room temperature. Slides were washed again then mounted by mounting solution from Sigma mixed with DAPI from Roche. The slides were then sealed and imaged the next day using a 20x objective lens on the Zeiss Observer Z1 microscope.

2.5 Cell Transfection with siRNA

Flexi Tubes siRNA for StarD13 oligo 3 and 8 obtained from Qiagen. The cells were transfected with the siRNA at a final concentration of 10 nM using Hiperfect (Qiagen) according to the manufacturer's specifications. Control cells were transfected with siRNA sequences targeting GL2 Luciferase (Qiagen). After 72 hours, protein levels in total cell lysates were analyzed by western blotting using the appropriate antibodies, or the effect of the corresponding knockdown was assessed.

2.6 Western ImmunoBlotting

Whole-cell lysates were prepared by scraping the cells with laemmli sample buffer containing 4% SDS, 20% glycerol, 10% β-mercaptoethanol, 0.004% bromophenol blue, and 0.125M Tris HCL (pH 6.8). SDS-PAGE was carried out under standard conditions and proteins were blotted onto a PVDF membrane. The membranes were then blocked with 5% bovine serum albumin for 1 hour and then incubated overnight at 4°C with either primary antibody against StarD13 (Abcam, 1:200 dilution) or actin (Abcam, 1:2500). After the incubation with the primary antibody, the membranes were washed and incubated 24 with a secondary antibody (Promega;1:1000) for 1 hour at room temperature. The membranes were then washed, and the bands visualized by treating the membranes with western blotting chemiluminescent reagent ECL (GE Healthcare). The levels of protein expression were compared by densitometry using the ImageJ software.

2.7 Sphere Formation Assay

DU145 cell suspension was placed on ice after trypsinization and centrifugation (1500 rpm for 5 min), then 2000 cells/condition were mixed with thawed Matrigel (Corning) in a 1:1 ratio. 100 µl of the master mix (Cells+Matrigel) were plated in a circular manner around the rim of each well of a 24 well-plate. Then the plate was incubated at 37 °C for 45-60 min for the Matrigel to solidify. 700 µl of warm 5% FBS RPMI-1640 AQ media were added in the middle of each well in addition to 100 µl of the transfection master mix (Opti-MEM (Gibco), Hiperfect (Qiagen), and the corresponding siRNA Luciferase, StarD13 oligo 3, and StarD13 oligo 8). After 3 days, the media is replenished, and the transfection master mix is added again, and so on for 13 days. Images were taken by a light microscope at 10x and quantified via ZEN for Image Analysis - Zeiss.

2.8 Sphere Immunoblotting

DU145 spheres were formed using the sphere formation assay (below) and collected in Eppendorf tubes. Then spheres were fixed with 4% PFA then permeabilized using 0.5% Triton X-1000 at room temperature. After that, spheres were blocked using the sphere blocking solution (0.1% BSA, 0.2% Triton X-1000, 0.05% Tween-20) for 2 hours. Spheres were then incubated with the primary anti-StarD13 over-night at 4 °C. The next day, spheres were washed gently with PBS containing 0.1% Tween-20 then incubated with the Alexa-488 conjugated secondary antibody for 2 hours. Spheres were gently washed again and pelleted. The pellet was then mixed with 5-7µl of anti-fade reagent mixed

with DAPI and mounted gently with a glass coverslip. Slides were sealed and imaged the next day at a 20x objective lens on the Zeiss Observer Z1 microscope.

2.9 Proliferation Assay

Cells were seeded in a 96-well plate and transfected with either siRNA targeting Luciferase or StarD13 siRNA and cell viability was determined using water-soluble cell proliferation reagent WST-1 (Roche, Mannheim, Germany). After the addition of WST-1 for 2 hours in a humidified incubator at 37 °C and 5% CO_2, the color change caused by the cleavage of the tetrazolium salt into formazan by mitochondrial dehydrogenases was measured using an ELISA reader at 450mm.

2.10 Motility Assay (Time-Lapse)

Cells were plated on a 35mm petri dish and transfected with si-Luciferase, si-StarD13. The assay was performed 72 hours after transfection. For motility analysis, cells were imaged in RPMI-1640 AQ (10% FBS, 1% non-essential amino acid) media, buffered using HEPES, and overlaid with mineral oil on a 37°C stage. Images were collected every 60 seconds for 2 hours using a 20X objective lens on the Zeiss Observer Z1 microscope. The speed of cell movement was quantified using the ROI tracker plugin in the ImageJ software, which was used to calculate the total distance traveled by individual cells. The speed is then calculated by dividing this distance by the time (120 minutes) and reported in μm/min. The speed of at least 15 cells for each condition was calculated. The net distance traveled by the cell was calculated by measuring the distance traveled between the first and the last frame.

2.11 Wound Healing Assay

Cells were grown to confluence on culture plates and a wound was made in the monolayer with a sterile pipette tip. After wounding, the cells were washed to remove debris and a new medium was added. Phase-contrast images of the wounded area were taken at 0 and 24 hours after wounding. Wound widths were measured at 11 different positions for each wound, and the average rate of wound closure was calculated in μm/hr using the ImageJ software.

2.12 Adhesion Assay

96-well plates were coated with collagen using Collagen Solution, Type I from rat tail (Sigma) overnight at 37 °C then washed with washing buffer (0.1% BSA in RPMI-1620 AQ media). The plates were then blocked with 0.5% BSA in RPMI-1620 AQ media at 37 °C in a CO_2 incubator for 1 hour. This was followed by washing the plates and chilling them on ice. Meanwhile, the cells were trypsinized and counted to $4x10^5$ cell/ml. 50 μl of cells were added in each well and incubated at 37°C in a CO_2 incubator for 30 minutes. The plates were then shaken and washed 3 times. Cells were then fixed with 4% PFA at room temperature for 10 minutes, washed, and stained with crystal violet (5 mg/ml in 2% ethanol) for 10 minutes. Following the staining, the plates were washed extensively with water and left to dry completely. Crystal violet was solubilized by incubating the cells with 2% SDS for 30 minutes. The absorption of the plates was read at 550 nm using an ELISA reader.

2.13 Immunocytochemistry

Cells were plated on glass coverslips and the appropriate treatment was applied. Cells were fixed with 4% paraformaldehyde for 10 minutes at 37°C and permeabilized with 0.5% Triton-X 10 for 15 minutes on ice. To decrease background fluorescence, cells were rinsed with 0.1 M glycine then incubated with 0.1 M glycine for 10 minutes. For blocking, cells were incubated with 1% filtered BSA in PBS for 1 hour. Samples were then stained with primary antibodies overnight at 4°C and with fluorophore-conjugated secondary antibodies for 1 hour. Fluorescent images were taken using a 63x objective lens on the Zeiss Observer Z1 microscope. Images were analyzed using Image J software.

2.14 Gelatin Invadopodia Assay

QCM Gelatin Invadopodia Assay (Green) kit from Sigma-Aldrich was used to measure the invasion ability of DU145 cells. Briefly, cells were plated on fluorescently labeled gelatin (matrix) and incubated at 37 °C and 5% CO_2 for 24 hours. Then cells were stained against Tks-4 (invadopodia marker) and visualized on a 63x objective lens of the Zeiss Observer Z1 microscope. The area devoid of fluorescence and intensity of the Tks -4 signal was analyzed using Image J software.

2.15 Quantification of Spheres

Using ZEN Image Analysis-Zeiss software, at least 50 spheres from each condition were quantified. The images were set to scale and the diameter of each

sphere was obtained through the circle tool to determine the diameter of each sphere.

2.16 Quantification of Focal Adhesions

Image J was used to quantify focal adhesions. Briefly, two main plugins were used to quantitate focal adhesions, CLAHE and Log3D. CLAHE enhances the local contrast of the image and Log3D filters the image based on user predefined parameters which allows detection and analysis of focal adhesions (Horzum, Ozdil, & Pesen-Okvur, 2014).

2.17 Statistical Analysis

The results reported represent average values from three independent experiments. The error estimates are given as ± SEM. The p-values were calculated by t-tests to check if the changes observed in the results were significant.

Chapter 3

Results

3.1 StarD13 Regulates Several Proteins and Cellular Processes

The literature was searched to develop a list of factors that interact and/or are regulated by StarD13 in different tumor types, and functional comparative analysis was done on the list of factors by PANTHER software (Table 1). The results showed that StarD13 interacts with proteins that have catalytic (cyclins, TAZ, ROCK, ERK, Cdc42, Rac1, FKBP51, RhoA,), binding (RhoA, Rac1, Cdc42, HOXB4, ROCK, CDH5, CTGF, cyclins, Bax), and regulatory (TAZ, Sox2, HOXB4, cyclins, paxillin) functions. Moreover, these proteins are involved in proliferation, biogenesis, development (ErbB2, RhoA, ERK, ROCK, Rac1, cyclins, paxillin, Sox2, HOXB4, CDH5, TP53INP1, etc.), adhesion (CTGF, paxillin, CDH5), and cell motility (Cdc42, paxillin, ERK, Rac1, RhoA) processes. (figure 11 & 12).

Table 1.StarD13 Targets Proteins in Several Tumor Types.

Cancer Type	STARD13 Modulated/Interacting Targets				
Brain	Cdc42, pERK, Rac, Rho A (El-Sitt et al., 2012; Khalil et al., 2014; Nicolas, Abdellatef, Haddad, Fakhoury, & El-Sibai, 2019)	VEGF-A (Nicolas, Abdellatef, Haddad, Fakhoury, & El-Sibai, 2019)			
Breast	Rho A, Rac (Hanna et al., 2014)	ErbB2 (Basak et al., 2018)	CDH5, HOXD1, HOXD10, Integrin, Vimentin, E-Cadherin (Zheng, Xiang et al., 2018)	RNPC1, CDH5, HOXD10, HOXD1 (Zheng, Zhang et al., 2018)	TP53INP1 (Zheng, Li et al., 2018)
	YAP, TAZ, Rho A, Rock, MLC, ALDH1, OCT3/4, Sox2, Nanog, CTGF, CDH5, HOXD1, HOXD10 (Zheng et al., 2018)	HOXB4, Rho A (Zhou, Liu, Xiong, & Sun, 2017)	BMF, Bax, Bcl-2 (Guo et al., 2018)	FKBP51 (Takaoka, Ito, Miki, & Nakanishi, 2017)	
Bone	PUM2 (Hu et al., 2018)				
Colon	p53, Bcl-2, Bax, Cdc42, Rac, Rho A (Nasrallah et al., 2014)	Cyclin D, Cyclin E, E-Cadherin, N-Cadherin, Vimentin (Yang et al., 2019)			
Liver	Fas (Zhang, Wang, & Hu, 2017)	Raf-1, ERK1/2, p70S6K, Paxillin (Leung, Yam, Chan, Ching, & Ng, 2010)	Rho A, pMLC-S19, YAP, CTGF, ALDH1, Nanog (Gao, Yu, Meng, Wang, & Jia, 2018)		
Prostate	E-cadherin N-cadherin Vimentin (Chen et al., 2019)				

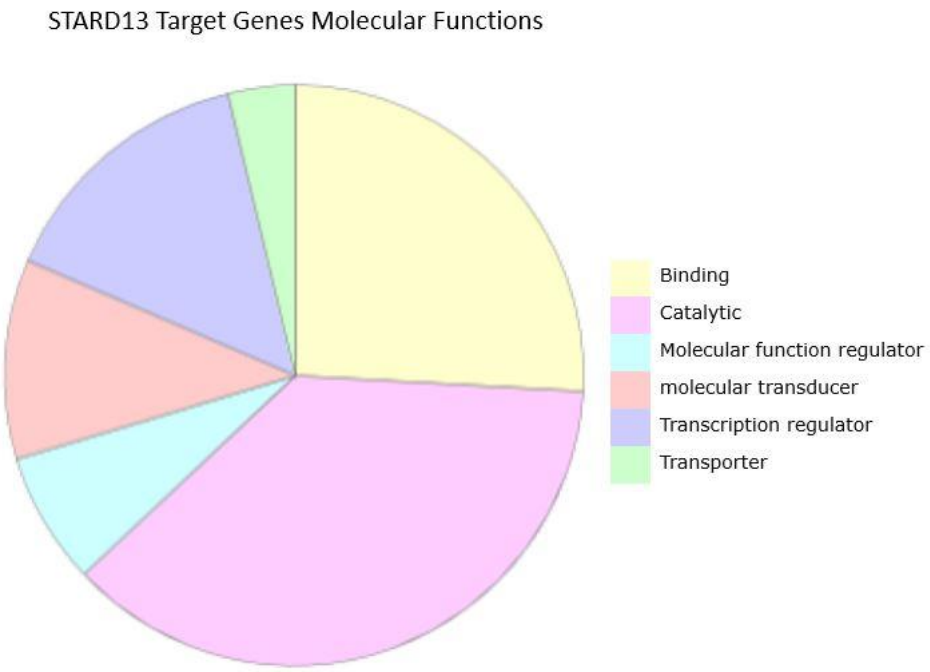

Figure 11. Biological Functions of StarD13 Targets. Ontology analysis was done by PANTHER.

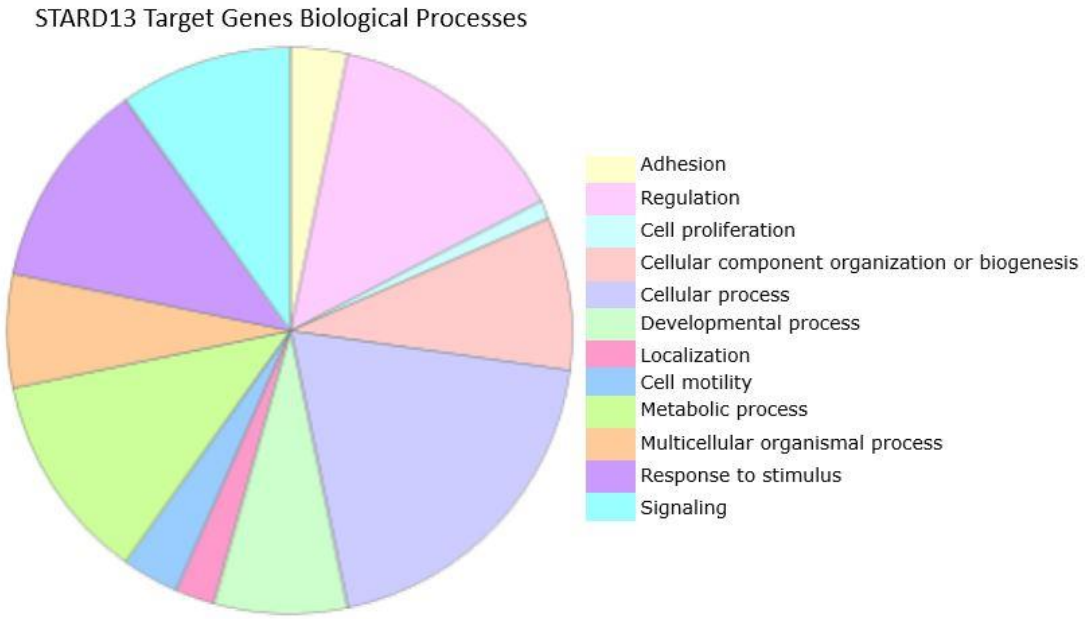

Figure 12. Biological Processes Performed by StarD13 Targets. Ontology Analysis was done by PANTHER.

3.2 StarD13 is Involved in Many Cellular Pathways

Pathways that involve StarD13 were determined and constructed by STRING software. It was found that proteins belonging to different structural and functional families are involved in biological pathways that are involved in proliferation and regulation of cell cycle (p38, cyclins, ERK, ErbB2), apoptosis (Bax, Bcl-2, p53, Fas), angiogenesis, stemness, and regulation of cytoskeleton dynamics (RhoA, Rac1, etc.) (figure 13 & 14). All these processes present the hallmarks of cancer development.

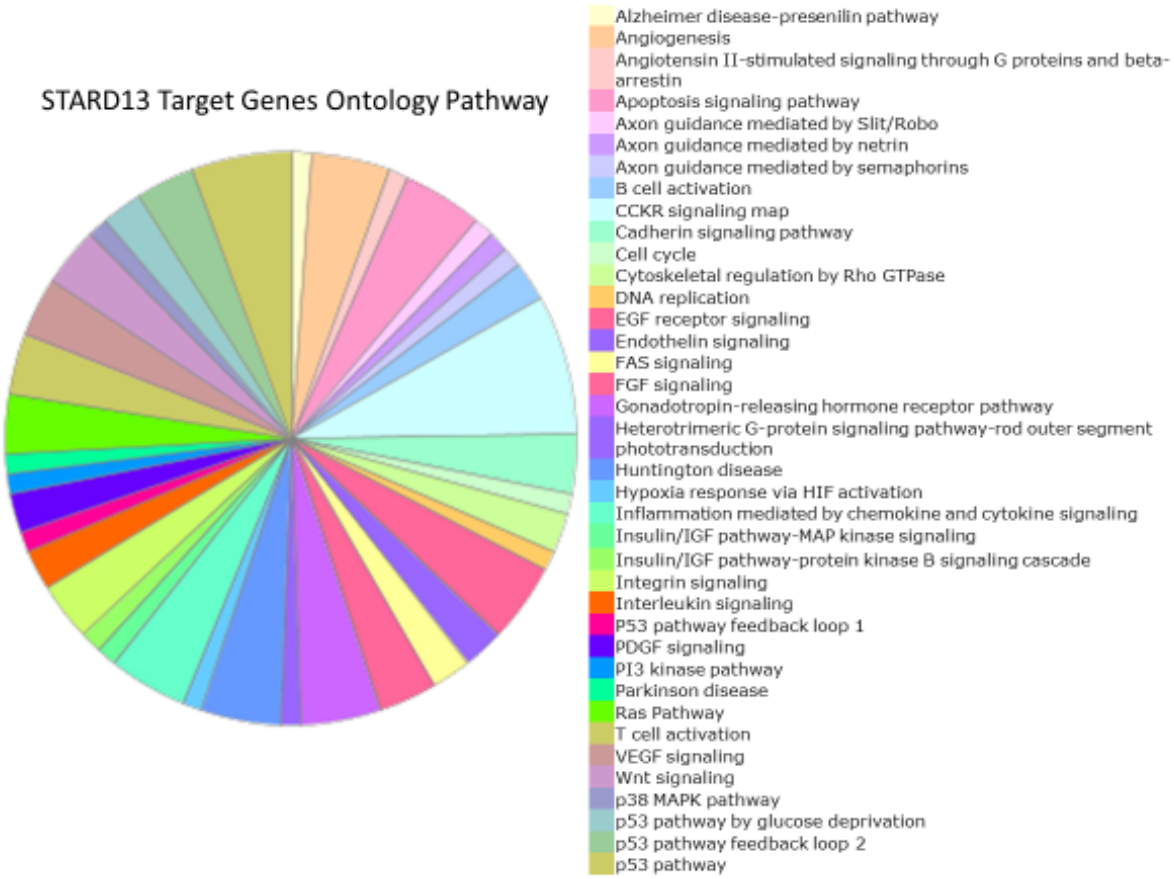

Figure 13. StarD13 Targets are Involved in Various Biological Pathways.

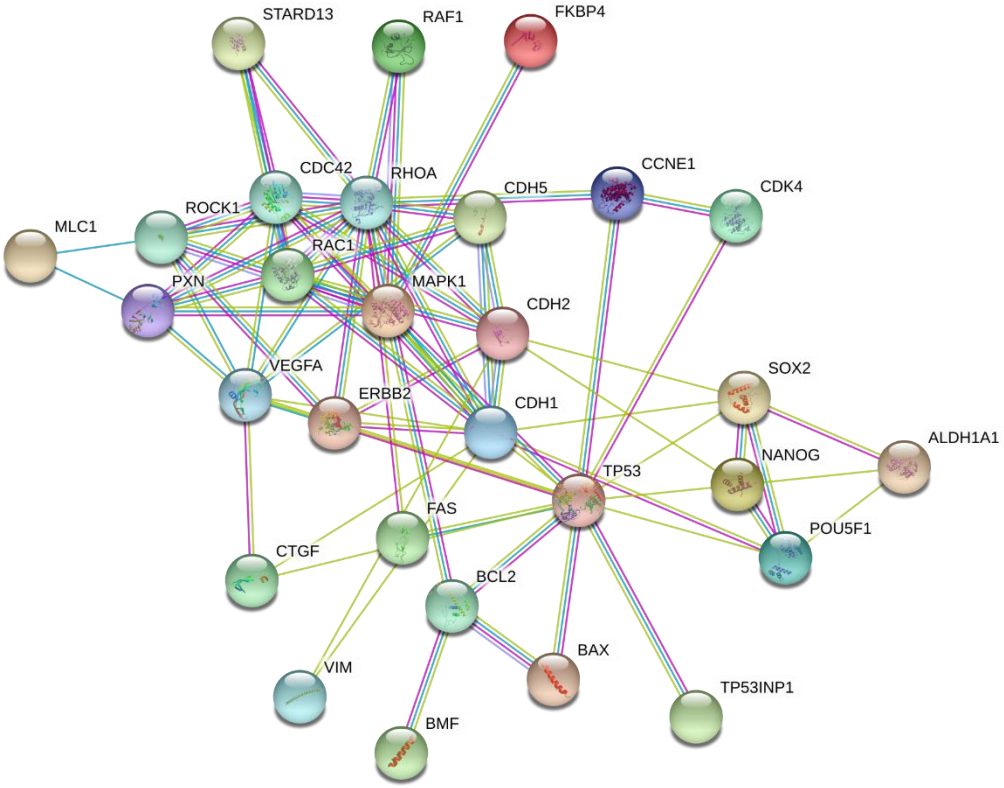

Figure 14. Networks Involving StarD13 and its Targets. Global pathway analysis of the 36 potential targets of StarD13 was performed using STRING database. The network nodes are proteins whose final position in the network is computed by minimization of the energy of the system. The color of the lines refers to the source predicting the active interaction. Green: texmining, pink: experimentally determined, and blue: curated databases.

3.3 StarD13 is Under Expressed in Prostate Cancer

Since StarD13 is involved in many pathways at the core of cancer development, the role of StarD13 in prostate cancer was of interest to us.

To establish the overall expression of StarD13 in prostate tissue, immunohistochemistry was performed on normal prostate tissue and a tissue corresponding to adenosis of the prostate, a low-grade prostate tumor. There was a 16% decrease in StarD13 signal intensity in the prostate cancer tissue when compared to the normal one. (figure 15)

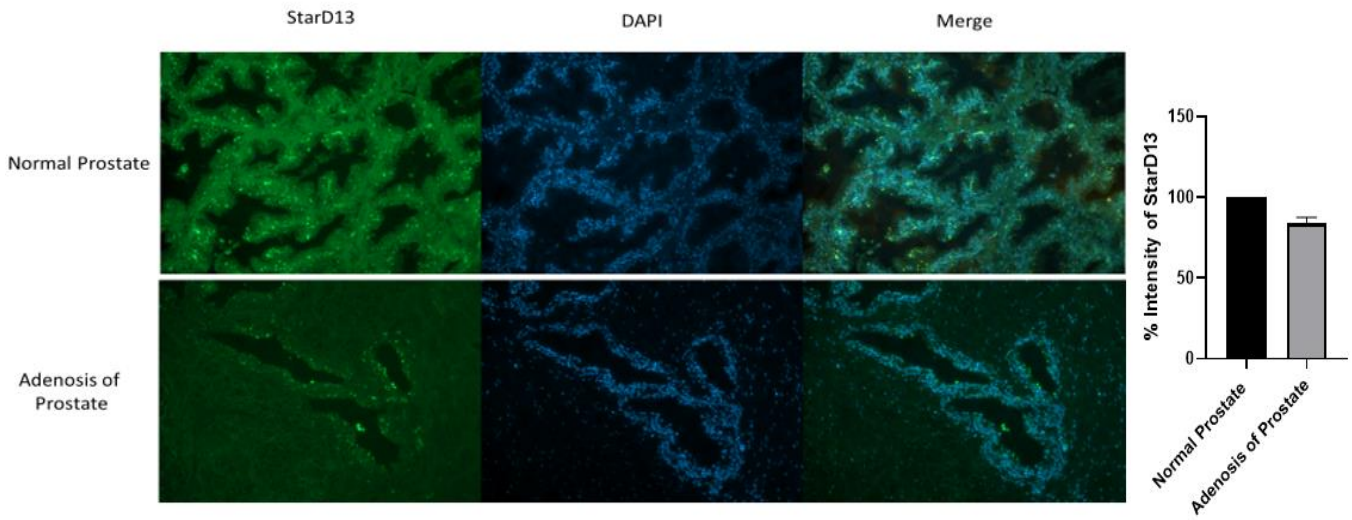

Figure 15. StarD13 is Under Expressed in Prostate Cancer. (A) Immunohistochemistry of normal prostate tissue (top micrograph) and adenosis of prostate tissue (lower micrograph) against StarD13 (green), DAPI (blue), and a merge image between StarD13 and DAPI. Tissue were visualized on a 20x lens of a fluorescent microscope. (B) Quantification of StarD13 expression using ImageJ software. Data are the mean -/+ SEM from 3 assays. The results were significant with $p<0.05$.

3.4 Silencing StarD13 by siRNA

To study the role of StarD13 in prostate cancer cell line DU145, StarD13 was knocked down by two oligonucleotides of si-StarD13, 3 and 8 in 2D and 3D DU145 cell cultures.

3.4.1 StarD13 Silencing in 2D DU145 Cell Culture

After transfecting the cells with the appropriate si-RNA, western immunoblotting against StarD13 was done to test the silencing efficiency of si-StarD13 oligonucleotides (3 and 8) compared to a nonspecific negative control (si-Luciferase), and actin as an endogenous control for loading.

The transfection of si-StarD13 oligo 3 and oligo 8 resulted in the reduction of StarD13 expression by 37% and 50% respectively in DU145 cells, compared to the control (si-Luciferase). (figure 16)

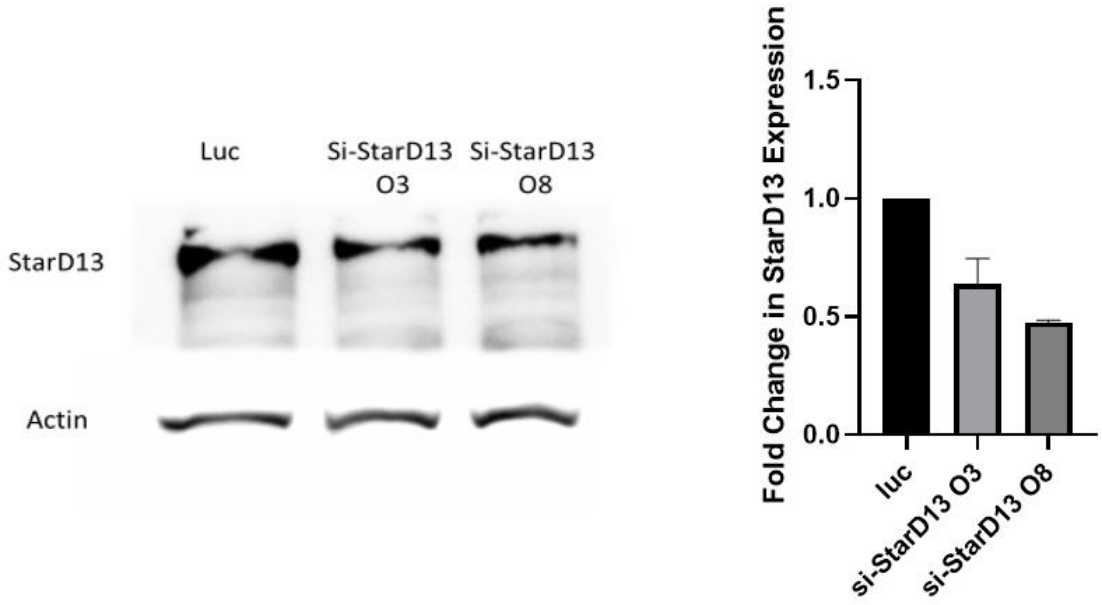

Figure 16. Efficient Depletion of StarD13 by si-RNA. DU145 cells were transfected with si-Luciferase, si-StarD13 oligo 3, or oligo 8 for 72 hours. Cells were lysed and blotted against StarD13. (A) Western blot profile showing the expression of StarD13 (upper lane) and actin (lower Lane). (B) Quantification of StarD13 expression by ImageJ software Data are the mean -/+ SEM from 3 assays. The results were significant with $p<0.05$.

3.4.2 StarD13 Silencing in 3D DU145 Cell Culture

Since 2D cell culture studies do not give a realistic view on the 3D tumor behavior, a knockdown efficiency test was done on DU145 spheres to verify the silencing capability of si-StarD13 oligo 3 and 8 compared to a non-specific control (luciferase) in 3D culture. After performing sphere formation assay followed by si-RNA transfection, the spheres were immunostained against StarD13 and the intensity of the signal was determined.

The results show a 65.4% and 68.8% reduction in StarD13 signal in Du145 spheres transfected with si-StarD13 oligo 3 and 8, respectively. These results were compared to non-specific control (si-Luciferase). (figure 17)

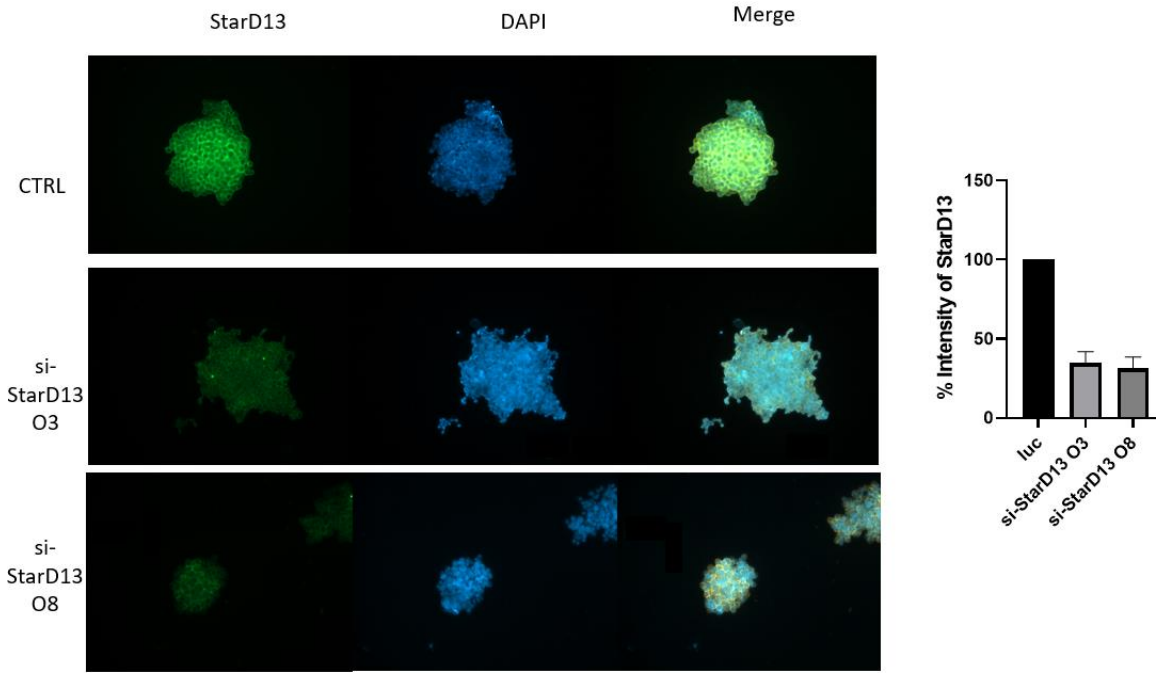

Figure 17. StarD13 is Silenced in DU145 Spheres by si-RNA. DU145 spheres were formed from DU145 cells transfected with si-Luciferase, si-StarD13 oligo 3, or oligo 8, then stained against StarD13 and visualized using a 64x lens of a fluorescent microscope. (A) Micrographs showing StarD13 expression (green) and DAPI stain (blue) after transfection si-Luciferase (upper panel), si-StarD13 oligo 3 (middle panel), and oligo 8 (lower panel). (B) Quantification of StarD13 signal intensity using ImageJ software. Data are the mean -/+ SEM from 3 assays. The results were significant with $p<0.05$.

3.5 StarD13 is a Tumor Suppressor

To establish the role of StarD13 in prostate cancer proliferation, two approaches were considered. The first one is measuring the proliferative activity of Du145 cells using the WST-1 reagent that reflects the metabolic activity of cells, and the second one is by measuring the area of 3D Du145 spheres that reflects the proliferative activity of a cell within a specific period.

3.5.1 StarD13 Suppresses Du145 Cell Proliferation

Proliferation assay was performed after silencing StarD13 using si-StarD13 oligo 3 and 8. This resulted in a 32% and 22% increase in DU145 cell

proliferation respectively when compared to the control (si-Luciferase). Cell viability was determined by WST-1 reagent. (figure 18)

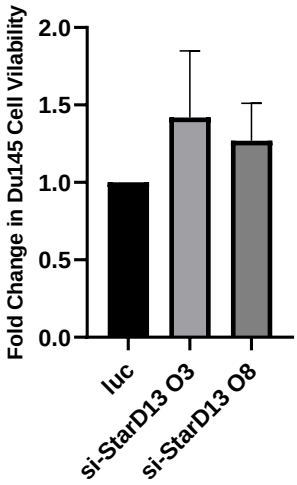

Figure 18.StarD13 Reduces Du145 Cell Proliferation in 2D Culture. Du145 cells were transfected with si-luciferase, si-StarD13 oligo 3, or oligo 8. Cell viability was measured by the color change of WST-1 at 450nm using ELISA plate reader. The Data are the mean -/+ SEM from three different trials. The results were significant with $p<0.05$.

3.5.2 StarD13 Reduces Du145 Sphere Formation Rate

To determine the effect of StarD13 on the rate of Du145 sphere formation which corresponds to the proliferative activity of this cell line, cells were transfected with si-StarD13 oligo 3 and 8 then sphere formation assay was performed. The area of single spheres from each condition was measured after 12 days.

Depletion of StarD13 using si-StarD13 oligo 3 and 8 led to a 66% and 38% increase in Du145 sphere area respectively when compared to the area of spheres transfected with si-Luciferase (control). (figure 19)

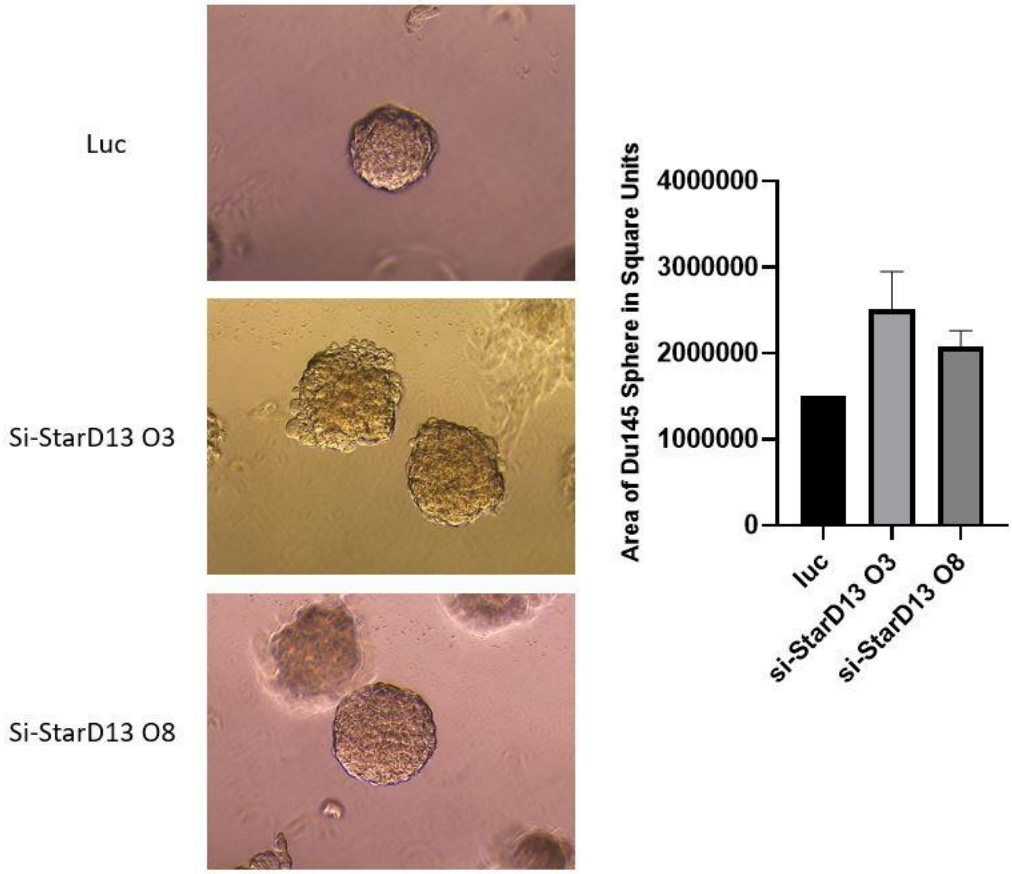

Figure 19. StarD13 Reduces DU145 Sphere Area. DU145 spheres were transfected with si-Luciferase, si-StarD13 oligo 3, or oligo 8, and images were taken using 10x lens after 12 days. (A) Sphere micrograph in si-Luciferase (upper panel), si-StarD13 oligo 3 (middle panel), and oligo 8 (lower panel). (B) quantification of area of spheres was done by ImageJ. The Data are the mean -/+ SEM from three different trials. The results were significant with $p<0.05$.

3.6 StarD13 is Required in Prostate Cancer Motility

The effect of StarD13 on cellular motility was identified using two approaches: time-lapse and wound healing assay, and in both assays, cell motility was determined to be reduced upon knocking down StarD13 by si-StarD13.

3.6.1 Effect of StarD13 on Cell Motility Measured by Time Lapse

The time-lapse assay measures the net movement of a cell over a specific period. It showed that, when compared to the control, the silencing of StarD13 led to a 43% and 53.8% decrease in net distance migrated by Du145 cells that were transfected by si-StarD13 oligo 3 and 8, respectively. (figure 20)

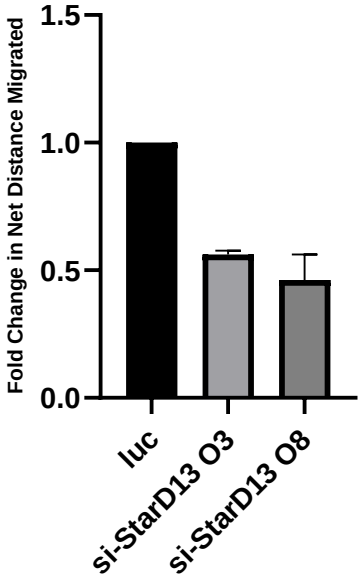

Figure 20. StarD13 Is a Positive Regulator of Cellular Motility. DU145 cells were transfected with Si-luciferase, Si-StarD13 oligo 3, or oligo 8 for 72 hours. The average migrated distance was quantitated using ImageJ software. The Data are the mean -/+ SEM from two different trials. The results were significant with $p<0.05$.

3.6.2 Effect of StarD13 on Cell Motility Measured by Wound-Healing Assay

A wound-healing assay was used to measure the migration rate of the cells to close the wound within 24 hours. This assay proved that upon knocking down StarD13 by si-StarD13 oligo 3 and oligo 8, the rate of wound closure by DU145 cells decreased by 45% and 51% respectively when compared to control (si-Luciferase). (figure 21).

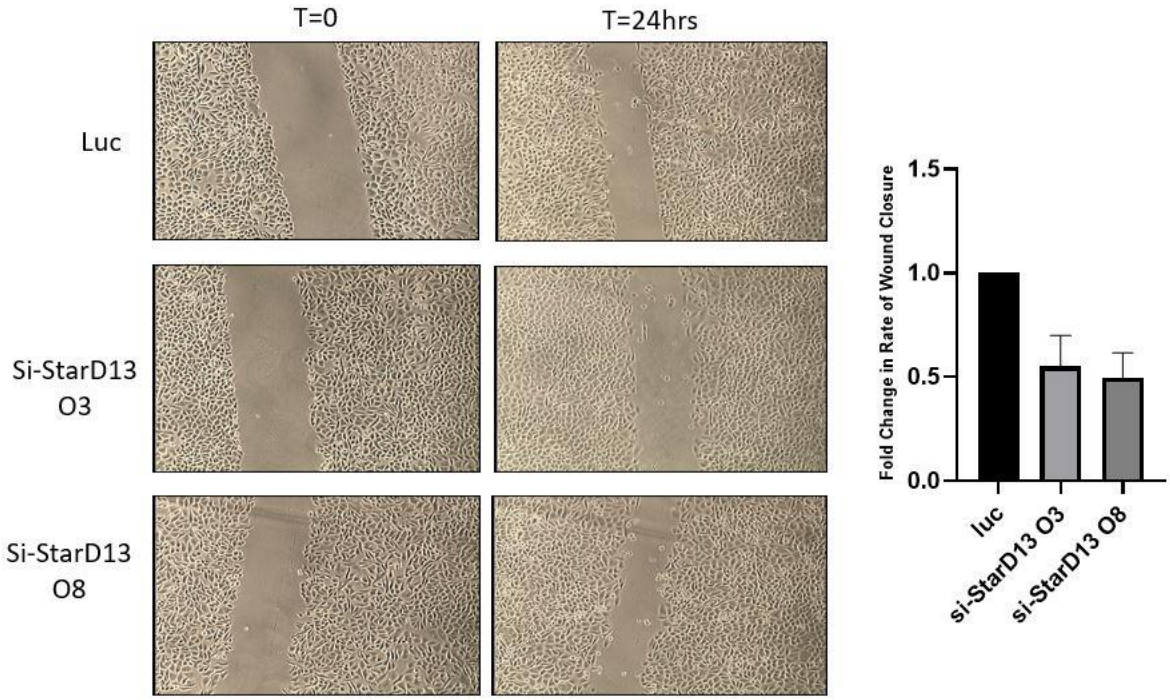

Figure 21. StarD13 Depletion Induces Wound Closure. DU145 cells were transfected with si-luciferase, si-StarD13 oligo 3, or oligo 8 for 72 hours. A wound is created, and images are taken in the same frame at t=o and after 24 hours. (A) Wound profile at t=o and t=24hrs in si-luciferase (upper panel), si-StarD13 oligo3 (middle panel), or oligo8 (lower panel). (B) Quantification of wound closure rate in fold changes from si-luciferase. Data are the mean -/+ SEM from 3 assays. The results were significant with $p<0.05$.

3.7 StarD13 is a Negative Regulator of Prostate Cancer Adhesion

According to the functional analysis results, one of the processes that are regulated by StarD13 is cellular adhesion. The Role of StarD13 in DU145 cell adhesion was identified using two approaches: immunoblotting for focal adhesions, and adhesion assay following StarD13 depletion using the two oligonucleotides.

3.7.1 StarD13 Reduces Overall Adhesion of DU145 Cells

To study the effect of StarD13 on DU145 cell adhesion to the extracellular matrix, StarD13 was silenced using si-StarD13 oligo 3 or 8 followed by plating DU145 cells on collagen that resembles the ECM in the tumor

microenvironment. This led to a 35% and 65% increase in cellular adhesion in the presence of si-StarD13 oligo 3 and 8, respectively. The results were compared to the non-specific negative control, si-Luciferase. (figure 22)

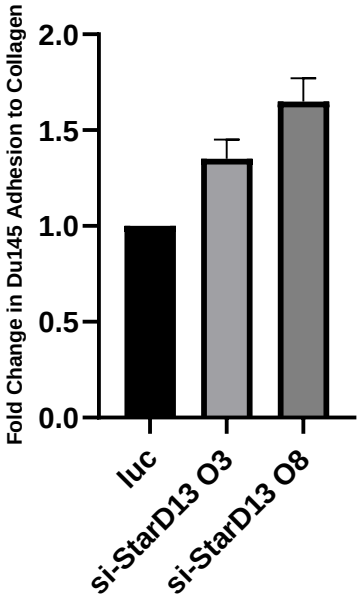

Figure 22. StarD13 is a Negative Regulator or DU145 Cell Adhesion to Collagen. DU145 cells were transfected with si-Luciferase, si-StarD13 oligo 3, or oligo 8 and plated on collagen. Crystal violet was solubilized using sodium dodecyl sulfate (SDS) and the absorption of the plates was read at 550μm using an ELISA plate reader. Data are the mean -/+ SEM from 2 assays. The results were significant with $p<0.05$.

3.7.2 StarD13 Reduces Focal Adhesions Count and Area

Focal adhesions are actin-rich structures that are used by the cell to adhere to the underlying matrix, and one of their markers is paxillin. So, to determine the role of StarD13 on the adhesion of prostate cancer, DU145 cells were stained with anti-paxillin antibody after knocking down StarD13 (Figure 23). Depletion of StarD13 by si-StarD13 oligo 3 and 8 led to a 9% and 8.2% increase in the area of focal adhesions respectively when compared to the non-specific control (Luciferase). Also, the Silencing of StarD13 using oligo 3 and 8 led to a 70% and

120% increase in the number of focal adhesions respectively when compared to Luciferase.

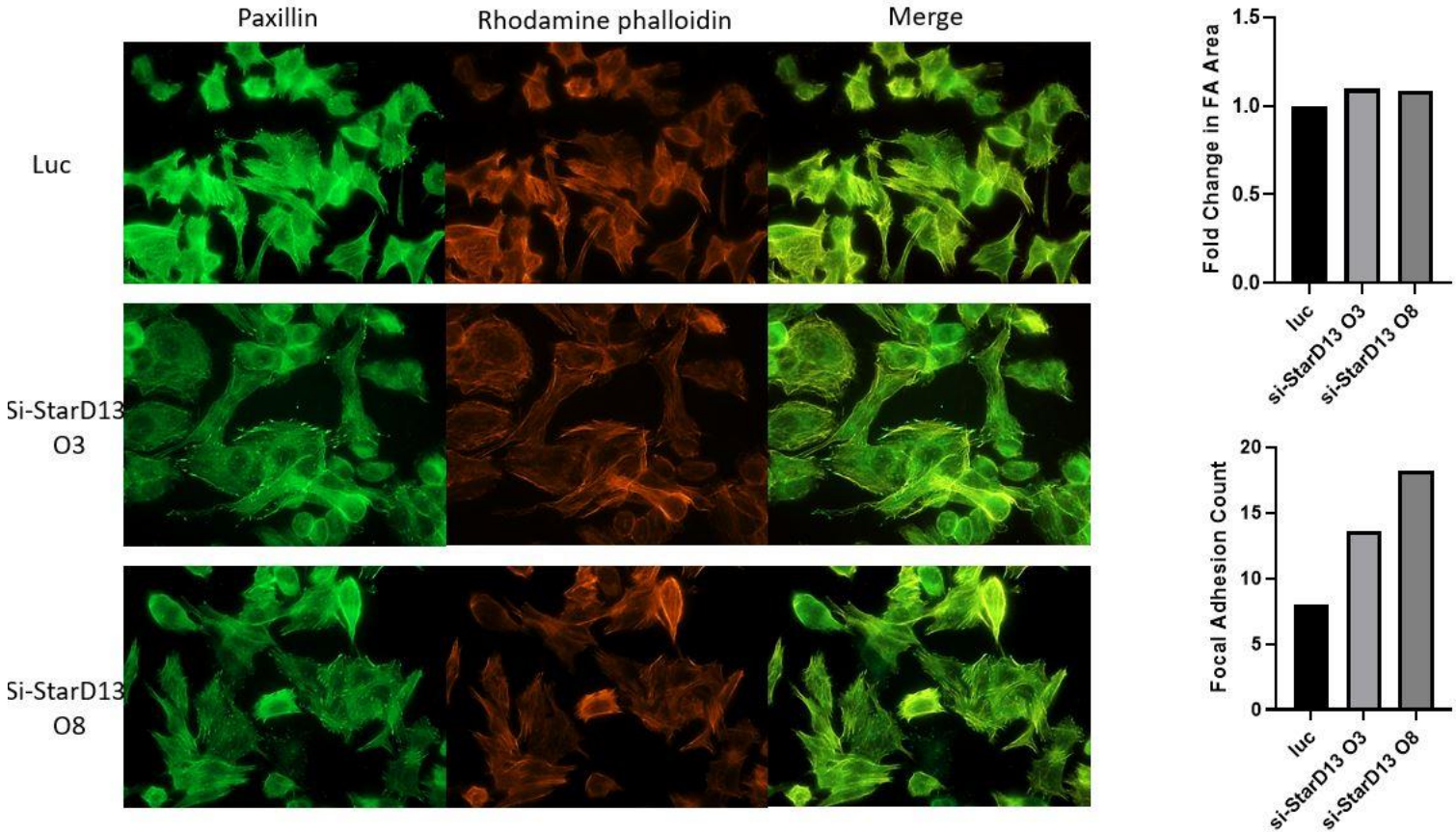

Figure 23. StarD13 Negatively Regulates Paxillin in Du145 Cells. (A) Representative micrographs of DU145 cells transfected with Si-luciferase (upper panel), Si-StarD13 oligo 3 (middle panel) and oligo 8 (lower panel) that were fixed and immunostained with paxillin (green) and Rhodamine phalloidin (orange). Cells were imaged using a 63x objective. (B) The area of focal adhesions and (C) the number of these focal adhesions were quantified using ImageJ.

3.8 StarD13 is a Negative Regulator of Prostate Cancer Invasion

To test the role of StarD13 on DU145 cells invasion, gelatin invadopodia assay was done. StarD13 was silenced and cells were plated on fluorescently labeled gelatin (matrix) then incubated at 37 °C and 5% CO_2 for 24 hours. The cells were then stained against Tks -4, a marker of invadopodia, and one of the

main factors needed for invadopodia assembly (Iizuka, Abdullah, Buschman, Diaz, & Courtneidge, 2016). Results showed that StarD13 depletion by si-StarD13 oligo 3 and 8 led to a 14% and 20% increase in invaded area by DU145, respectively. Moreover, the intensity of the Tks-4 signal increases by 15% and 13.4% in DU145 cells upon knocking down StarD13 using oligos 3 and 8 respectively. All results were in comparison to the non-specific control, si-Luciferase. (figure 24)

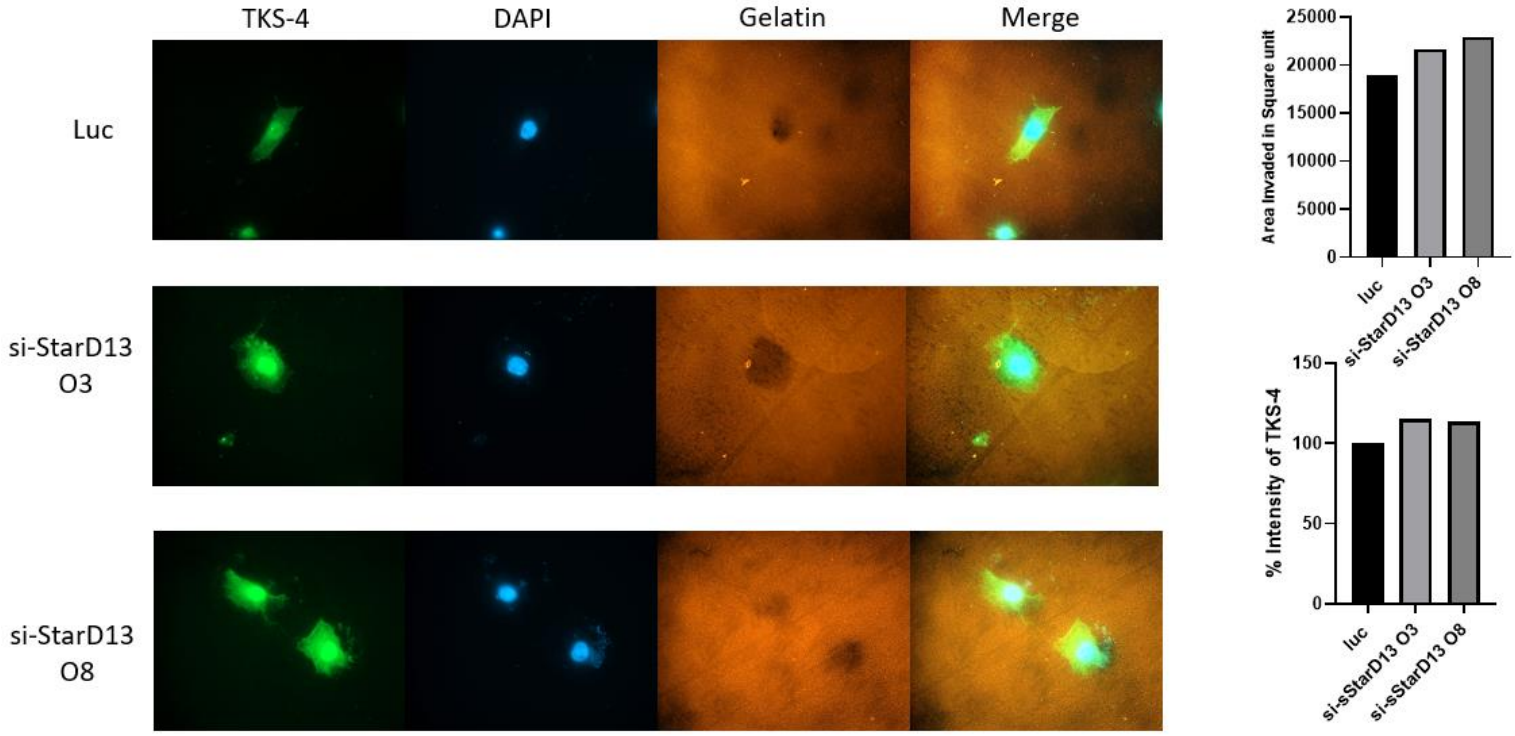

Figure 24 StarD13 Silencing Enhances DU145 Cell Invasion. DU145 cells were transfected with si-Luciferase, si-StarD13 oligo3, or oligo 8 and plated on fluorescently labeled gelatin, then cells were stained against Tks-4 as a marker of invadopodia. (A) Micrographs showing the change in invaded area (orange), intensity of Tks-4 (green), and DAPI (blue) in DU145 cells transfected by si-Luciferase (upper panel), si-STarD13 oligo 3 (middle panel), and oligo 8 (lower panel). (B) Quantification of area invaded by DU145 cells. (C) Quantification of the intensity of Tks-4 signals in DU145 cells. Images were visualized using a 64x lens of a fluorescent microscope and quantified using ImageJ software.

Chapter 4

Discussion

StarD13 is admitted to be a tumor suppressor gene in various tumor types such as breast cancer, astrocytoma, colorectal cancer, and hepatocellular carcinoma (Basak et al., 2018; El-Sitt et al., 2012; Hanna et al., 2014; Zhang, Wang, & Hu, 2017). However, it is found to be under-expressed in tumors due to gene deletions, epigenetics, or copy loss (Hankins et al., 2008; Tayrac et al., 2009; Wang et al., 2016). The localization of StarD13 and its different domains make this protein a multitasking factor in the different aspects of cancer malignancy such as proliferation, motility, and invasion (Ching et al., 2003; Li, X. et al., 2016; Yang, B. et al., 2019; Zheng et al., 2018). In this study, we present an overall view on the role of StarD13 in prostate cancer proliferation, motility, adhesion, and invasion.

The literature was inspected to create a list of the genes that StarD13 regulates or interacts with, in seven cancer types. Then, a functional comparative analysis was done to classify these factors according to their function, the processes they are involved in, and the pathways they run trough. We determined that StarD13 target genes that are ramified in functions including binding, catalysis, regulation, signal transduction, epigenetic modulation, and molecular export. Then we established that StarD13 interact/regulate factors that are involved in cellular proliferation, biogenesis, adhesion, apoptosis, angiogenesis, inflammation, and cell motility which is mainly regulated by the family of Rho GTPases. Also, these pathways indicate the presence of interactions between StarD13 and Rho A which is in line with the GAP function of StarD13. A lot of

these biological processes represent the hallmarks of cancer, which guides us to the importance of StarD13 in cancer development and malignancy. StarD13 is found to suppress cancer development mainly through its SAM and GAP domains, and to our knowledge, in prostate cancer, the literature only showed the interaction of StarD13 with N-cadherins, E-cadherins, and vimentin that are markers of EMT (Chen, L. et al., 2019), but not other proteins. That is why, we decided to elaborate on the role of StarD13 as a Rho GAP in prostate cancer proliferation, migration, and invasion.

First, the overall expression of StarD13 was determined in normal prostate tissue and adenosis of prostate tissue that represents a low-grade prostate cancer sample. It was determined that there is a substantial decrease in StarD13 expression in the cancer tissue when compared to the normal one. This is in concordance with other studies in the literature on other tumor types (Ullmannova & Popescu, 2006).

To assess the role of StarD13 in prostate cancer, the DU145 cell line was considered as an in vitro model of prostate cancer. To determine the effect of StarD13 on cellular proliferation, WST-1 proliferation assay was done after silencing StarD13 using si-RNA. StarD13 depletion led to an increase in cell viability. Further on, to establish a realistic image on the role of StarD13 in cell proliferation, DU145 spheres, presenting 3D prostate cancer cell culture, were formed from cells transfected with the appropriate si-RNA targeting StarD13. This assay showed an increase in sphere area in the absence of StarD13 which correlates to a faster cellular division in a specific time (12 days). These two approaches, proliferation and sphere formation assays, showed that StarD13 plays a tumor suppressor role in prostate cancer as the case in other tumor types established in previous studies (El-Sitt et al., 2012; Hanna et al., 2014).

Since cancer metastasis is the leading cause of the poor prognosis of this disease, it is interesting to elaborate on the role of StarD13 in prostate cancer metastasis. Metastasis is a multistep process that depends on cellular motility, adhesion, and invasion (Zeeshan & Mutahir, 2017). To learn the effect of StarD13 on DU145 cell motility, net distance migrated in 2 hours and the rate of wound closure by prostate cells was measured after StarD13 depletion. In both assays, cell motility appeared to decrease in the absence of StarD13, and although StarD13 is determined as a tumor suppressor, here it shows that StarD13 is needed for 2D cell migration. This Data is consistent with previous studies done in our lab on breast cancer, astrocytoma, and colorectal cancer (El-Sitt et al., 2012; Hanna et al., 2014; Nasrallah et al., 2014).

The first step in cancer metastasis is the downregulation of adhesion proteins that render the cell detached from the tumor and the surrounding environment (Lu, Jiang, Blume-Jensen, & Hunter, 2001; Okabe et al., 2018; Tang et al., 2019). This fact raised our interest in the effect of StarD13 on focal adhesion proteins and the process of adhesion to a substrate in general. Therefore, adhesion assay was performed, and it showed that the ability of DU145 cells to attach to collagen increases upon knocking down StarD13. Also, DU145 cells stained against paxillin, a marker of focal adhesions, showed an increase in the number of focal adhesions that were of bigger areas after StarD13 silencing. This implicates that StarD13 hinders prostate cancer adhesion to the underlying matrix. This claim seems to contradict the previous result showing the positive regulation of 2D motility by StarD13 since cellular motility depends on the cycle of adhesion and detachment from the ECM. However, the contradiction could be explained by the fact that StarD13 is a Rho GAP to Rho A that is responsible for focal

adhesion formation, and the under-expression of StarD13 leads to the constitutive activation of Rho A resulting in enhanced adhesion to the substrate and reduced motility (Hanna et al., 2014). Also, since cell motility is a cycle of attaching to the ECM at the front end and detaching at the rear end, looking at the localization of StarD13 in a motile cell may be a potential way to explain this paradigm.

Following detachment from its surroundings, the cancer cell tends to express and secrete metalloprotease enzymes through their invadopodia structures that degrade the extracellular matrix and allow the cell to reach blood or lymphatic vessels that serve as transporters to distant locations (Zeeshan & Mutahir, 2017). So, we wanted to determine the role of StarD13 on prostate cancer invasive ability, and gelatin invadopodia assay was performed. The depletion of StarD13 led to the increase in the area of gelatin (matrix) degraded by DU145 cells and the upregulation of the invadopodia marker Tks-4 expression, which means that there is an increase in invadopodia formation (Iizuka et al., 2016; Saini & Courtneidge, 2018). These results highlight the negative role that StarD13 plays in the prostate cancer 3D motility (invasion). This result is in concordance with the tumor suppressor role played by StarD13 in prostate cancer, however, it opposes the findings on the effect of StarD13 in 2D cellular motility in the same tumor. These findings are consistent with previous studies on the effect of StarD13 on cellular invasion in different tumor types (El-Sitt et al., 2012; Hanna et al., 2014; Nasrallah et al., 2014).

Chapter 5

Conclusion

StarD13 is found to be involved in many aspects of cancer malignancy including proliferation, biogenesis, angiogenesis, and cell motility. In this study, we identified the role of StarD13 in prostate cancer. We showed that StarD13 is underexpressed in prostate cancer tumors and that it acts as a tumor suppressor through the downregulation of cellular proliferation in 2D and 3D cultures. Also, we elaborated on the role of StarD13 in the different steps of cancer metastasis whereby, we found that StarD13 is a positive attributor to 2D cell motility but not 3D motility presented by cellular invasion to the underlying matrix through invadopodia formation. Moreover, StarD13 is found to play a negative role in the regulation of adhesion and focal adhesion formation. This Data shows that even though StarD13 acts as a proliferation, adhesion, and invasion suppressor, it positively contributes to the 2D cellular motility which is among the main assets of cancer malignancy.

In the future, we are interested in testing the role of Star13 in prostate cancer formation which is related to cancer stemness. Also, we want to elaborate on the crosstalk between the family of Rho GTPases and StarD13 in the formation of invadopodia and focal adhesions in prostate cancer cells. We are also interested in looking at the role of StarD13 in prostate cancer invasion in a 3D spheroid system that would give a closer picture of the tumor behavior inside the body.

References

Alblazi, K. M. O., & Siar, C. H. (2015). Cellular protrusions--lamellipodia, filopodia, invadopodia and podosomes--and their roles in progression of orofacial tumours: Current understanding. *Asian Pacific Journal of Cancer Prevention: APJCP, 16*(6), 2187-2191. doi:10.7314/apjcp.2015.16.6.2187

Bailly, M., & Condeelis, J. (2002). Cell motility: Insights from the backstage. *Nature Cell Biology, 4*(12), 292. doi:10.1038/ncb1202-e292

Bajaj, J., Diaz, E., & Reya, T. (2020). Stem cells in cancer initiation and progression. *Journal of Cell Biology, 219*(1) doi:10.1083/jcb.201911053

Bamburg, J. R. (1999). Proteins of the ADF/cofilin family: Essential regulators of actin dynamics. *Annual Review of Cell and Developmental Biology, 15*, 185-230. doi:10.1146/annurev.cellbio.15.1.185

Basak, P., Leslie, H., Dillon, R. L., Muller, W. J., Raouf, A., & Mowat, M. R. A. (2018). In vivo evidence supporting a metastasis suppressor role for Stard13 (Dlc2) in ErbB2 (neu) oncogene induced mouse mammary tumors. *Genes, Chromosomes & Cancer, 57*(4), 182-191. doi:10.1002/gcc.22519

Beaty, B. T., & Condeelis, J. (2014). Digging a little deeper: The stages of invadopodium formation and maturation. *European Journal of Cell Biology, 93*(10), 438-444. doi:10.1016/j.ejcb.2014.07.003

Beli, P., Mascheroni, D., Xu, D., & Innocenti, M. (2008). WAVE and Arp2/3 jointly inhibit filopodium formation by entering into a complex with mDia2. *Nature Cell Biology, 10*(7), 849-857. doi:10.1038/ncb1745

Braun, A. C., & Olayioye, M. A. (2015). Rho regulation: DLC proteins in space and time. *Cellular Signalling, 27*(8), 1643-1651. doi:10.1016/j.cellsig.2015.04.003

Bravo-Cordero, J. J., Magalhaes, M. A. O., Eddy, R. J., Hodgson, L., & Condeelis, J. (2013). Functions of cofilin in cell locomotion and invasion. *Nature Reviews Molecular Cell Biology, 14*(7), 405-415. doi:10.1038/nrm3609

Cancer facts & figures 2020 | american cancer society. Retrieved from https://www.cancer.org/research/cancer-facts-statistics/all-cancer-facts-figures/cancer-facts-figures-2020.html

Carvalho-Santos, Z., Azimzadeh, J., Pereira-Leal, J. B., & Bettencourt-Dias, M. (2011). Evolution: Tracing the origins of centrioles, cilia, and flagella. *The Journal of Cell Biology, 194*(2), 165-175. doi:10.1083/jcb.201011152

Cerroni, L., Barnhill, R., Elder, D., Gottlieb, G., Heenan, P., Kutzner, H., . . . Kerl, H. (2010). Melanocytic tumors of uncertain malignant potential: Results of a tutorial held at the XXIX symposium of the international society of dermatopathology in graz, october 2008. *The American Journal of Surgical Pathology, 34*(3), 314-326. doi:10.1097/PAS.0b013e3181cf7fa0

Chen, L., Hu, W., Li, G., Guo, Y., Wan, Z., & Yu, J. (2019). Inhibition of miR-9-5p suppresses prostate cancer progress by targeting StarD13. *Cellular & Molecular Biology Letters, 24*, 20. doi:10.1186/s11658-019-0145-1

Chen, N., & Zhou, Q. (2016). The evolving gleason grading system. *Chinese Journal of Cancer Research, 28*(1), 58-64. doi:10.3978/j.issn.1000-9604.2016.02.04

Cheng, L., Montironi, R., Bostwick, D. G., Lopez-Beltran, A., & Berney, D. M. (2012). Staging of prostate cancer. *Histopathology, 60*(1), 87-117. doi:10.1111/j.1365-2559.2011.04025.x

Ching, Y., Wong, C., Chan, S., Leung, T. H., Ng, D. C., Jin, D., & Ng, I. O. (2003). Deleted in liver cancer (DLC) 2 encodes a RhoGAP protein with growth suppressor function and is underexpressed in hepatocellular carcinoma. *The Journal of Biological Chemistry, 278*(12), 10824-10830. doi:10.1074/jbc.M208310200

Christofori, G. (2006). New signals from the invasive front. *Nature, 441*(7092), 444-450. doi:10.1038/nature04872

Dagogo-Jack, I., & Shaw, A. T. (2018). Tumour heterogeneity and resistance to cancer therapies. *Nature Reviews. Clinical Oncology, 15*(2), 81-94. doi:10.1038/nrclinonc.2017.166

Deng, G., Krishnakumar, S., Powell, A. A., Zhang, H., Mindrinos, M. N., Telli, M. L., . . . Jeffrey, S. S. (2014). Single cell mutational analysis of PIK3CA in circulating tumor cells and metastases in breast cancer reveals heterogeneity, discordance, and mutation persistence in cultured disseminated tumor cells from bone marrow. *BMC Cancer, 14*, 456. doi:10.1186/1471-2407-14-456

Dickover, M., Hegarty, J. M., Ly, K., Lopez, D., Yang, H., Zhang, R., . . . Chi, N. C. (2014). The atypical rho GTPase, RhoU, regulates cell-adhesion molecules during cardiac morphogenesis. *Developmental Biology, 389*(2), 182-191. doi:10.1016/j.ydbio.2014.02.014

Eddy, R. J., Weidmann, M. D., Sharma, V. P., & Condeelis, J. S. (2017). Tumor cell invadopodia: Invasive protrusions that orchestrate metastasis. *Trends in Cell Biology, 27*(8), 595-607. doi:10.1016/j.tcb.2017.03.003

El Atat, O., Fakih, A., & El-Sibai, M. (2019). RHOG activates RAC1 through CDC42 leading to tube formation in vascular endothelial cells. *Cells, 8*(2) doi:10.3390/cells8020171

El-Sitt, S., & El-Sibai, M. (2013). The STAR of the DLC family. *Journal of Receptor and Signal Transduction Research, 33*(1), 10-13. doi:10.3109/10799893.2012.752002

El-Sitt, S., Khalil, B. D., Hanna, S., El-Sabban, M., Fakhreddine, N., & El-Sibai, M. (2012). DLC2/StarD13 plays a role of a tumor suppressor in astrocytoma. *Oncology Reports, 28*(2), 511-518. doi:10.3892/or.2012.1819

Etienne-Manneville, S., & Hall, A. (2002). Rho GTPases in cell biology. *Nature, 420*(6916), 629-635. doi:10.1038/nature01148

Fares, J., Fares, M. Y., Khachfe, H. H., Salhab, H. A., & Fares, Y. (2020). Molecular principles of metastasis: A hallmark of cancer revisited. *Signal Transduction and Targeted Therapy, 5*(1), 1-17. doi:10.1038/s41392-020-0134-x

Figure 1: Steps of the cell motility cycle. | nature reviews molecular cell biology. Retrieved from https://www.nature.com/articles/nrm3609/figures/1

Folkman, J. (1995). Angiogenesis in cancer, vascular, rheumatoid and other disease. *Nature Medicine, 1*(1), 27-30. doi:10.1038/nm0195-27

Fritz-Laylin, L. K., Lord, S. J., & Mullins, R. D. (2017). WASP and SCAR are evolutionarily conserved in actin-filled pseudopod-based motility. *The Journal of Cell Biology, 216*(6), 1673-1688. doi:10.1083/jcb.201701074

Galkin, V. E., Orlova, A., Kudryashov, D. S., Solodukhin, A., Reisler, E., Schröder, G. F., & Egelman, E. H. (2011). Remodeling of actin filaments by ADF/cofilin proteins. *Proceedings of the National Academy of Sciences of the United States of America, 108*(51), 20568-20572. doi:10.1073/pnas.1110109108

Garnham, R., Scott, E., Livermore, K. E., & Munkley, J. (2019). ST6GAL1: A key player in cancer (review). *Oncology Letters, 18*(2), 983-989. doi:10.3892/ol.2019.10458

Génot, E., & Gligorijevic, B. (2014). Invadosomes in their natural habitat. *European Journal of Cell Biology, 93*(10), 367-379. doi:10.1016/j.ejcb.2014.10.002

Gorovoy, M., Niu, J., Bernard, O., Profirovic, J., Minshall, R., Neamu, R., & Voyno-Yasenetskaya, T. (2005). LIM kinase 1 coordinates microtubule stability and actin polymerization in human endothelial cells. *The Journal of Biological Chemistry, 280*(28), 26533-26542. doi:10.1074/jbc.M502921200

Guo, X., Xiang, C., Zhang, Z., Zhang, F., Xi, T., & Zheng, L. (2018). Displacement of bax by BMF mediates STARD13 3'UTR-induced breast cancer cells apoptosis in an miRNA-depedent manner. *Molecular Pharmaceutics, 15*(1), 63-71. doi:10.1021/acs.molpharmaceut.7b00727

Gupta, G. P., & Massagué, J. (2006). Cancer metastasis: Building a framework. *Cell, 127*(4), 679-695. doi:10.1016/j.cell.2006.11.001

Haga, R. B., & Ridley, A. J. (2016). Rho GTPases: Regulation and roles in cancer cell biology. *Small GTPases, 7*(4), 207-221. doi:10.1080/21541248.2016.1232583

Hanahan, D., & Weinberg, R. A. (2000). The hallmarks of cancer. *Cell, 100*(1), 57-70. doi:10.1016/S0092-8674(00)81683-9

Hanahan, D., & Weinberg, R. A. (2011). Hallmarks of cancer: The next generation. *Cell, 144*(5), 646-674. doi:10.1016/j.cell.2011.02.013

Hankins, G. R., Sasaki, T., Lieu, A., Saulle, D., Karimi, K., Li, J. Z., & Helm, G. A. (2008). Identification of the deleted in liver cancer 1 gene, DLC1, as a candidate meningioma tumor suppressor. *Neurosurgery, 63*(4), 771-781. doi:10.1227/01.NEU.0000325488.72518.9E

Hanna, S., & El-Sibai, M. (2013). Signaling networks of rho GTPases in cell motility. *Cellular Signalling, 25*(10), 1955-1961. doi:10.1016/j.cellsig.2013.04.009

Hanna, S., Khalil, B., Nasrallah, A., Saykali, B. A., Sobh, R., Nasser, S., & El-Sibai, M. (2014). StarD13 is a tumor suppressor in breast cancer that regulates cell motility and invasion. *International Journal of Oncology, 44*(5), 1499-1511. doi:10.3892/ijo.2014.2330

Harris, E. S., Li, F., & Higgs, H. N. (2004). The mouse formin, FRLalpha, slows actin filament barbed end elongation, competes with capping protein, accelerates polymerization from monomers, and severs filaments. *The Journal of Biological Chemistry, 279*(19), 20076-20087. doi:10.1074/jbc.M312718200

Heasman, S. J., & Ridley, A. J. (2008). Mammalian rho GTPases: New insights into their functions from in vivo studies. *Nature Reviews. Molecular Cell Biology, 9*(9), 690-701. doi:10.1038/nrm2476

Higashida, C., Miyoshi, T., Fujita, A., Oceguera-Yanez, F., Monypenny, J., Andou, Y., . . . Watanabe, N. (2004). Actin polymerization-driven molecular movement of mDia1 in living cells. *Science (New York, N.Y.), 303*(5666), 2007-2010. doi:10.1126/science.1093923

Hiraga, T. (2018). Hypoxic microenvironment and metastatic bone disease. *International Journal of Molecular Sciences, 19*(11) doi:10.3390/ijms19113523

Horzum, U., Ozdil, B., & Pesen-Okvur, D. (2014). Step-by-step quantitative analysis of focal adhesions. *MethodsX, 1*, 56-59. doi:10.1016/j.mex.2014.06.004

Idikio, H. A. (2011). Human cancer classification: A systems biology- based model integrating morphology, cancer stem cells, proteomics, and genomics. *Journal of Cancer, 2*, 107-115. Retrieved from https://www.ncbi.nlm.nih.gov/pmc/articles/PMC3072616/

Iizuka, S., Abdullah, C., Buschman, M. D., Diaz, B., & Courtneidge, S. A. (2016). The role of tks adaptor proteins in invadopodia formation, growth and metastasis of melanoma. *Oncotarget, 7*(48), 78473-78486. doi:10.18632/oncotarget.12954

Information, National Center for Biotechnology, Pike, U. S. National Library of Medicine 8600 Rockville, MD, B., & Usa, 2. (2020). *Localized prostate cancer: Overview* Institute for Quality and Efficiency in Health Care (IQWiG). Retrieved from https://www.ncbi.nlm.nih.gov/books/NBK284958/

Jaafar, L., Chamseddine, Z., & El-Sibai, M. (2020). StarD13: A potential star target for tumor therapeutics. *Human Cell*, doi:10.1007/s13577-020-00358-2

Jacob, A., & Prekeris, R. (2015). The regulation of MMP targeting to invadopodia during cancer metastasis. *Frontiers in Cell and Developmental Biology, 3*, 4. doi:10.3389/fcell.2015.00004

Kawai, K., Seike, J., Iino, T., Kiyota, M., Iwamae, Y., Nishitani, H., & Yagisawa, H. (2009). START-GAP2/DLC2 is localized in focal adhesions via its N-terminal region. *Biochemical and Biophysical Research Communications, 380*(4), 736-741. doi:10.1016/j.bbrc.2009.01.095

Key statistics for prostate cancer | prostate cancer facts. Retrieved from https://www.cancer.org/cancer/prostate-cancer/about/key-statistics.html

Khalil, B. D., Hanna, S., Saykali, B. A., El-Sitt, S., Nasrallah, A., Marston, D., . . . El-Sibai, M. (2014). The regulation of RhoA at focal adhesions by StarD13 is important for astrocytoma cell motility. *Experimental Cell Research, 321*(2), 109-122. doi:10.1016/j.yexcr.2013.11.023

Kühn, S., & Geyer, M. (2014). Formins as effector proteins of rho GTPases. *Small GTPases, 5*, e29513. doi:10.4161/sgtp.29513

Kumar, S., Das, A., Barai, A., & Sen, S. (2018). MMP secretion rate and inter-invadopodia spacing collectively govern cancer invasiveness. *Biophysical Journal, 114*(3), 650-662. doi:10.1016/j.bpj.2017.11.3777

Kwak, E. L., Ahronian, L. G., Siravegna, G., Mussolin, B., Borger, D. R., Godfrey, J. T., . . . Corcoran, R. B. (2015). Molecular heterogeneity and receptor coamplification

drive resistance to targeted therapy in MET-amplified esophagogastric cancer. *Cancer Discovery, 5*(12), 1271-1281. doi:10.1158/2159-8290.CD-15-0748

Kwan, J. J., & Donaldson, L. W. (2007). The NMR structure of the murine DLC2 SAM domain reveals a variant fold that is similar to a four-helix bundle. *BMC Structural Biology, 7*, 34. doi:10.1186/1472-6807-7-34

Lämmermann, T., & Sixt, M. (2009). Mechanical modes of 'amoeboid' cell migration. *Current Opinion in Cell Biology, 21*(5), 636-644. doi:10.1016/j.ceb.2009.05.003

Lauffenburger, D. A., & Horwitz, A. F. (1996). Cell migration: A physically integrated molecular process. *Cell, 84*(3), 359-369. doi:10.1016/s0092-8674(00)81280-5

Li, W., Chong, H., & Guan, K. L. (2001). Function of the rho family GTPases in ras-stimulated raf activation. *The Journal of Biological Chemistry, 276*(37), 34728-34737. doi:10.1074/jbc.M103496200

Li, X., Zheng, L., Zhang, F., Hu, J., Chou, J., Liu, Y., . . . Xi, T. (2016). STARD13-correlated ceRNA network inhibits EMT and metastasis of breast cancer. *Oncotarget, 7*(17), 23197-23211. doi:10.18632/oncotarget.8099

Loeb, L. A., Springgate, C. F., & Battula, N. (1974). Errors in DNA replication as a basis of malignant changes. *Cancer Research, 34*(9), 2311-2321.

Loeb, L. A. (2011). Human cancers express mutator phenotypes: Origin, consequences and targeting. *Nature Reviews. Cancer, 11*(6), 450-457. doi:10.1038/nrc3063

Loeb, L. A., Loeb, K. R., & Anderson, J. P. (2003). Multiple mutations and cancer. *Proceedings of the National Academy of Sciences of the United States of America, 100*(3), 776-781. doi:10.1073/pnas.0334858100

Lu, Z., Jiang, G., Blume-Jensen, P., & Hunter, T. (2001). Epidermal growth factor-induced tumor cell invasion and metastasis initiated by dephosphorylation and downregulation of focal adhesion kinase. *Molecular and Cellular Biology, 21*(12), 4016-4031. doi:10.1128/MCB.21.12.4016-4031.2001

Ma, X., Dang, Y., Shao, X., Chen, X., Wu, F., & Li, Y. (2019). Ubiquitination and long non-coding RNAs regulate actin cytoskeleton regulators in cancer progression. *International Journal of Molecular Sciences, 20*(12) doi:10.3390/ijms20122997

McGranahan, N., & Swanton, C. (2017). Clonal heterogeneity and tumor evolution: Past, present, and the future. *Cell, 168*(4), 613-628. doi:10.1016/j.cell.2017.01.018

Michaelis, U. R. (2014). Mechanisms of endothelial cell migration. *Cellular and Molecular Life Sciences: CMLS, 71*(21), 4131-4148. doi:10.1007/s00018-014-1678-0

Moshfegh, Y., Bravo-Cordero, J. J., Miskolci, V., Condeelis, J., & Hodgson, L. (2015). A trio-Rac1-Pak1 signalling axis drives invadopodia disassembly. *Nature Cell Biology, 17*(3), 350. doi:10.1038/ncb3123

Murphy, D. A., & Courtneidge, S. A. (2011). The 'ins' and 'outs' of podosomes and invadopodia: Characteristics, formation and function. *Nature Reviews Molecular Cell Biology, 12*(7), 413-426. doi:10.1038/nrm3141

Nasrallah, A., Saykali, B., Al Dimassi, S., Khoury, N., Hanna, S., & El-Sibai, M. (2014). Effect of StarD13 on colorectal cancer proliferation, motility and invasion. *Oncology Reports, 31*(1), 505-515. doi:10.3892/or.2013.2861

Nguyen, K., Sabata, B., & Jain, A. K. (2012). Prostate cancer grading: Gland segmentation and structural features. *Pattern Recognit. Lett.*, doi:10.1016/j.patrec.2011.10.001

Nicolas, S., Abdellatef, S., Haddad, M. A., Fakhoury, I., & El-Sibai, M. (2019). Hypoxia and EGF stimulation regulate VEGF expression in human glioblastoma multiforme (GBM) cells by differential regulation of the PI3K/rho-GTPase and MAPK pathways. *Cells, 8*(11) doi:10.3390/cells8111397

Ohori, M., Wheeler, T. M., & Scardino, P. T. (1994). The new american joint committee on cancer and international union against cancer TNM classification of prostate cancer. clinicopathologic correlations. *Cancer, 74*(1), 104-114. doi:10.1002/1097-0142(19940701)74:13.0.co;2-5

Okabe, H., Aoki, K., Yogosawa, S., Saito, M., Marumo, K., & Yoshida, K. (2018). Downregulation of CD24 suppresses bone metastasis of lung cancer. *Cancer Science, 109*(1), 112-120. doi:10.1111/cas.13435

Pantel, K., & Speicher, M. R. (2016). The biology of circulating tumor cells. *Oncogene, 35*(10), 1216-1224. doi:10.1038/onc.2015.192

Pastushenko, I., & Blanpain, C. (2019). EMT transition states during tumor progression and metastasis. *Trends in Cell Biology, 29*(3), 212-226. doi:10.1016/j.tcb.2018.12.001

Pollard, T. D., & Borisy, G. G. (2003). Cellular motility driven by assembly and disassembly of actin filaments. *Cell, 112*(4), 453-465. doi:10.1016/s0092-8674(03)00120-x

Rawla, P. (2019). Epidemiology of prostate cancer. *World Journal of Oncology, 10*(2), 63-89. doi:10.14740/wjon1191

Ridley, A. J. (2011). Life at the leading edge. *Cell, 145*(7), 1012-1022. doi:10.1016/j.cell.2011.06.010

Rossman, K. L., Der, C. J., & Sondek, J. (2005). GEF means go: Turning on RHO GTPases with guanine nucleotide-exchange factors. *Nature Reviews. Molecular Cell Biology, 6*(2), 167-180. doi:10.1038/nrm1587

Saini, P., & Courtneidge, S. A. (2018). Tks adaptor proteins at a glance. *Journal of Cell Science, 131*(1) doi:10.1242/jcs.203661

Satheesh, V., Chidambaranathan, P., Jagannadham, P. T., Kumar, V., Jain, P. K., Chinnusamy, V., . . . Srinivasan, R. (2016). Transmembrane START domain proteins: In silico identification, characterization and expression analysis under stress conditions in chickpea (cicer arietinum L.). *Plant Signaling & Behavior, 11*(2), e992698. doi:10.4161/15592324.2014.992698

Seth, A., Otomo, C., & Rosen, M. K. (2006). Autoinhibition regulates cellular localization and actin assembly activity of the diaphanous-related formins FRLalpha and mDia1. *The Journal of Cell Biology, 174*(5), 701-713. doi:10.1083/jcb.200605006

Sharma, V., Eddy, R., Entenberg, D., Kai, M., Gertler, F., & Condeelis, J. (2013). Tks5 and SHIP2 regulate invadopodium maturation, but not initiation, in breast carcinoma cells. *Current Biology, 23*(21), 2079-2089. doi:10.1016/j.cub.2013.08.044

Shi, R., Feng, W., Zhang, C., Yu, T., Fan, Z., Liu, Z., . . . Zhu, D. (2018). In vivo imaging the motility of monocyte/macrophage during inflammation in diabetic mice. *Journal of Biophotonics, 11*(5), e201700205. doi:10.1002/jbio.201700205

Sousa-Squiavinato, A. C. M., Rocha, M. R., Barcellos-de-Souza, P., de Souza, W. F., & Morgado-Diaz, J. A. (2019). Cofilin-1 signaling mediates epithelial-mesenchymal transition by promoting actin cytoskeleton reorganization and cell-cell adhesion regulation in colorectal cancer cells. *Biochimica Et Biophysica Acta. Molecular Cell Research, 1866*(3), 418-429. doi:10.1016/j.bbamcr.2018.10.003

Stengel, K., & Zheng, Y. (2011). Cdc42 in oncogenic transformation, invasion, and tumorigenesis. *Cellular Signalling, 23*(9), 1415-1423. doi:10.1016/j.cellsig.2011.04.001

Sun, L., Sun, J., & Song, J. (2019). High expression of DLC family proteins predicts better prognosis and inhibits tumor progression in NSCLC. *Molecular Medicine Reports, 19*(6), 4881-4889. doi:10.3892/mmr.2019.10146

Tan, B. T., Park, C. Y., Ailles, L. E., & Weissman, I. L. (2006). The cancer stem cell hypothesis: A work in progress. *Laboratory Investigation, 86*(12), 1203-1207. doi:10.1038/labinvest.3700488

Tang, H., Jiang, L., Zhu, C., Liu, R., Wu, Y., Yan, Q., . . . Guan, X. (2019). Loss of cell adhesion molecule L1 like promotes tumor growth and metastasis in esophageal

squamous cell carcinoma. *Oncogene, 38*(17), 3119-3133. doi:10.1038/s41388-018-0648-7

Tayrac, M. d., Etcheverry, A., Aubry, M., Saïkali, S., Hamlat, A., Quillien, V., . . . Mosser, J. (2009). Integrative genome-wide analysis reveals a robust genomic glioblastoma signature associated with copy number driving changes in gene expression. *Genes, Chromosomes and Cancer, 48*(1), 55-68. doi:10.1002/gcc.20618

Ullmannova, V., & Popescu, N. C. (2006). Expression profile of the tumor suppressor genes DLC-1 and DLC-2 in solid tumors. *International Journal of Oncology, 29*(5), 1127-1132.

Vega, F. M., & Ridley, A. J. (2008). Rho GTPases in cancer cell biology. *FEBS Letters, 582*(14), 2093-2101. doi:10.1016/j.febslet.2008.04.039

Vitiello, E., Ferreira, J. G., Maiato, H., Balda, M. S., & Matter, K. (2014). The tumour suppressor DLC2 ensures mitotic fidelity by coordinating spindle positioning and cell-cell adhesion. *Nature Communications, 5*, 5826. doi:10.1038/ncomms6826

Wang, D., Qian, X., Rajaram, M., Durkin, M. E., & Lowy, D. R. (2016). DLC1 is the principal biologically-relevant down-regulated DLC family member in several cancers. *Oncotarget, 7*(29), 45144-45157. doi:10.18632/oncotarget.9266

Watanabe, N., Kato, T., Fujita, A., Ishizaki, T., & Narumiya, S. (1999). Cooperation between mDia1 and ROCK in rho-induced actin reorganization. *Nature Cell Biology, 1*(3), 136-143. doi:10.1038/11056

Watanabe, N., Madaule, P., Reid, T., Ishizaki, T., Watanabe, G., Kakizuka, A., . . . Narumiya, S. (1997). p140mDia, a mammalian homolog of drosophila diaphanous, is a target protein for rho small GTPase and is a ligand for profilin. *The EMBO Journal, 16*(11), 3044-3056. doi:10.1093/emboj/16.11.3044

Worthylake, R. A., Lemoine, S., Watson, J. M., & Burridge, K. (2001). RhoA is required for monocyte tail retraction during transendothelial migration. *The Journal of Cell Biology, 154*(1), 147-160. doi:10.1083/jcb.200103048

Wu, A., Loutherback, K., Lambert, G., Estévez-Salmerón, L., Tlsty, T. D., Austin, R. H., & Sturm, J. C. (2013). Cell motility and drug gradients in the emergence of resistance to chemotherapy. *Proceedings of the National Academy of Sciences, 110*(40), 16103-16108.

Yamaguchi, H., & Condeelis, J. (2007). Regulation of the actin cytoskeleton in cancer cell migration and invasion. *Biochimica Et Biophysica Acta (BBA) - Molecular Cell Research, 1773*(5), 642-652. doi:10.1016/j.bbamcr.2006.07.001

Yamaguchi, H., Pixley, F., & Condeelis, J. (2006). Invadopodia and podosomes in tumor invasion. *European Journal of Cell Biology, 85*(3-4), 213-218. doi:10.1016/j.ejcb.2005.10.004

Yang, B., Zhou, S., Tan, J., Huang, J., Chen, Z., Zhong, G., & Han, F. (2019). Long non-coding RNA STARD13-AS suppresses cell proliferation and metastasis in colorectal cancer. *OncoTargets and Therapy, 12*, 9309-9318. doi:10.2147/OTT.S217094

Yang, Z., Chen, H., Shu, M., Zhang, Y., Xue, L., & Lin, Y. (2019). DLC2 operates as a tumor suppressor gene in breast cancer via the RhoGTPase pathway. *Oncology Letters, 17*(2), 2107-2116. doi:10.3892/ol.2018.9874

Yayoshi-Yamamoto, S., Taniuchi, I., & Watanabe, T. (2000). FRL, a novel formin-related protein, binds to rac and regulates cell motility and survival of macrophages. *Molecular and Cellular Biology, 20*(18), 6872-6881. doi:10.1128/mcb.20.18.6872-6881.2000

Yuan, Y. (2016). Spatial heterogeneity in the tumor microenvironment. *Cold Spring Harbor Perspectives in Medicine, 6*(8) doi:10.1101/cshperspect.a026583

Zeeshan, R., & Mutahir, Z. (2017). Cancer metastasis - tricks of the trade. *Bosnian Journal of Basic Medical Sciences, 17*(3), 172-182. doi:10.17305/bjbms.2017.1908

Zhang, H., Wang, F., & Hu, Y. (2017). STARD13 promotes hepatocellular carcinoma apoptosis by acting as a ceRNA for fas. *Biotechnology Letters, 39*(2), 207-217. doi:10.1007/s10529-016-2253-6

Zhao, L., Xu, G., Zhou, J., Xing, H., Wang, S., Wu, M., . . . Ma, D. (2006). The effect of RhoA on human umbilical vein endothelial cell migration and angiogenesis in vitro. *Oncology Reports, 15*(5), 1147-1152.

Zheng, L., Li, X., Chou, J., Xiang, C., Guo, Q., Zhang, Z., . . . Xi, T. (2018). StarD13 3'-untranslated region functions as a ceRNA for TP53INP1 in prohibiting migration and invasion of breast cancer cells by regulating miR-125b activity. *European Journal of Cell Biology, 97*(1), 23-31. doi:10.1016/j.ejcb.2017.11.002